Alma Mater Studiorum - Università di Bologna

SCUOLA DI SCIENZE

Dipartimento di Chimica Industriale"Toso Montanari"

Corso di Laurea Magistrale in

Chimica Industriale

Classe LM-71 - Scienze e Tecnologie della Chimica Industriale

A DFT study on chemodivergent synthesis of functionalized heterocycles

Tesi di laurea sperimentale

CANDIDATO

Filippo Silvestrini

RELATORE

Prof. Dr. Andrea Mazzanti

CORRELATORE

Dr. Michele Mancinelli

Daniel Pecorari

Anno Accademico 2018-2019

Riassunto

L'argomento di questa tesi è lo studio computazionale dei meccanismi di reazione per la sintesi di piperidine chirali 3,4,5-trisostituite e di morfoline 2,6-disostituite. La strategia sintetica consiste nell'uso dello stesso substrato per entrambe le sintesi. Esso contiene due siti nucleofili: un estere α,β-insaturo e un chetone, i quali evolvono differentemente in base al tipo di nucleofilo utilizzato (cianuro o-, fenilsolfuro) attraverso reazioni di addizione e ciclizzazione. Il catalizzatore utilizzato è un sale d'ammonio quaternario il quale, porta ad un eccesso diasteromerico sia per i prodotti morfolinci che per i prodotti piperidinici. Dallo studio tramite calcoli quantomeccanici delle reazioni è stato possibile dare una spiegazione alla chemoselettività ed alla diasteroselezione derivante dai due nucleofili utilizzati. Nel caso dei prodotti piperidinici è stato inoltre possibile validare l'ipotesi di meccanismo concertato di addizione nucleofila sul sito α,β-insaturo e ciclizzazione tramite addizione di Michael.

Abstract

The topic of this thesis is the DFT computational study of the mechanisms for the synthesis of chiral 3,4,5-trisubstituted piperidines and 2,6-disubstituted morpholines. The goal of this synthesis is to use, the same substrate containing two electrophilic sites: an α,β-unsaturated ester and a ketone, which evolves according to the nucleophile used (cyanide, phenyl sulfide) through different addition and cyclization reactions. A quaternary ammonium salt is used as a catalyst for these reactions, which leads to a diastereoisomeric excess both for the reactions of morpholine and piperidine products. Studies *in silico* of the pathways of these reactions explain the chemoselection and diasteroselection deriving from the two nucleophiles used. In this case of piperidine products, it was also possible to validate the hypothesis of a concerted nucleophilic addition mechanism on the α,β-unsaturated site and cyclization due to an intramolecular Michael addition.

Summary

1- Introduction

In recent years, the development of computers hardware and the increase in computational power led to an improvement in computational methods for chemistry. The ability to combine computational calculations with experimental evidence not only allow for confirmation of the experimental data obtained but, in many cases, adds for more information on the characteristics of the chemical system evaluated. In addition, to the simulation of molecular characteristics such as spectroscopic or thermodynamic properties, nowadays computational chemistry provides the tools for assessing the evolution of chemical reactions and useful information can be obtained about mechanisms that lead to product formation. In organic chemistry study, the most widely used calculation method is Density functional Theory (DFT). The molecular systems studied are usually of considerable size, so calculation methods based on Hartree-Fock theory, Rayleigh-Schrödinger (time-independent) perturbation theory, or the multiconfigurational methods are not an effective way to get results in a reasonable amount of time. One of the most widely computational level used for its excellent results in the DFT theory is the B3LYP/6-31G(d), that allows obtaining results in good agreement with the experimental one without requiring prohibitive calculation times. In some cases, however, the presence of dispersive forces and intramolecular interactions in the analyzed system can lead to the choice of other functionals rather than B3LYP. In this work, as in many recent DFT[1] studies for the evaluation of reaction mechanisms, it has been necessary to use another functional to more accurately assess the electronic energy of the system. The choice fell on the M06-2X functional coupled with the 6-311+G (d) basis set. What is usually done is to calculate electronic energy at the M06-2X/6-311+G(d) level and add to it the corrective contribution on the enthalpies calculated to a lower level of theory, in this case, B3LYP/6-31G(d). This computational strategy has been widely used in literature in recent years, the respective acronym being SMD-M06-2X/6-311+G(d)//B3LYP/6-31G(d). In one of their works, Houk and coworkers[2] found a nine-member cyclical transition state structure that justifies the stereoselectivity of aldolic reactions catalyzed by neighboring diamines. In another article by Goodman et al,[3] computational simulations allowed them to find a mechanism that explains the hydrogenation of imine through Hantzsch's ester, catalyzed by BINOL chiral analogs and phosphoric acids, and the enantioselection obtained. In this thesis, a computational study was chosen to carry out the reaction mechanism for two nucleophile additions involving the same substrate. Experimental evidence has shown that,

with a substrate containing two electrophile capabilities, the nature of the nucleophile determines which sites of the substrate will be the first target. The two nucleophiles can be considered as soft and hard, phenyl-sulfide and cyanide respectively, according to the hard-soft acids bases (HSAB) principle.[4] The two electrophile reaction sites of the substrate (see Figure 1) are the carbonyl of the ketone function (C=O) and the β carbon of the α,β-unsaturated ester system.

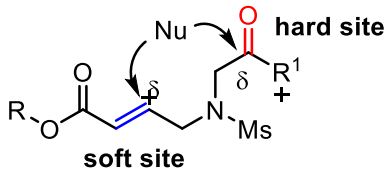

Figure 1- Typology of substrates with two electrophilic sites studied in this work.

1.1- Piperidines

Piperidines are six-term saturated heterocycles where there is a nitrogen. These substances are important building blocks in many synthetic procedures as they are present in many biologically active molecules. It is of great interest to obtain functionalized and optically active piperidines because different stereoisomer can interact differently in a biological environment. Several stereoisomers of the same molecule can go from being pharmacologically active to inactive only by varying the configuration of a stereogenic center. Figure 2 shows the piperidine molecule A and the same examples of its derivatives: molecule B is paroxetine, an antidepressant agent on serotonin receptors and an inhibitor of serotonin reuptake in the synaptic valley. Molecule C is methylphenidate, a drug widely used to treat attention deficit hyperactivity disorder (ADHD). Molecule D is fentanyl, one of the most selling synthetic opioid analgesic drugs in America, despite the side effects.

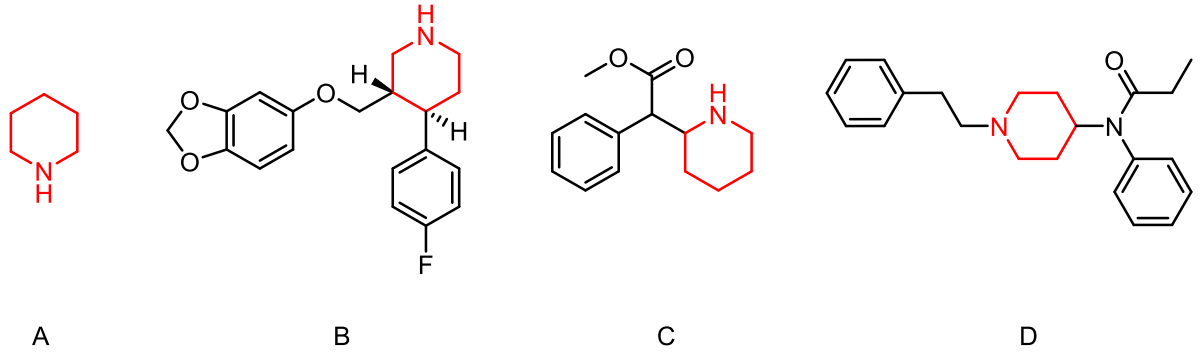

Figure 2- Some examples of piperidine derivatives.

The most commonly used synthetic methods for obtaining functionalized piperidines are (see Scheme 1): pyridine reduction reactions (Scheme 1a),[5] ring expansion reactions from 3-hydroxypyrrolidine (Scheme 1b)[6] or cascade addition-carbocyclization reactions, using a boronic acid as nucleophiles and a special Michael acceptor as electrophile (Scheme 1c).[7]

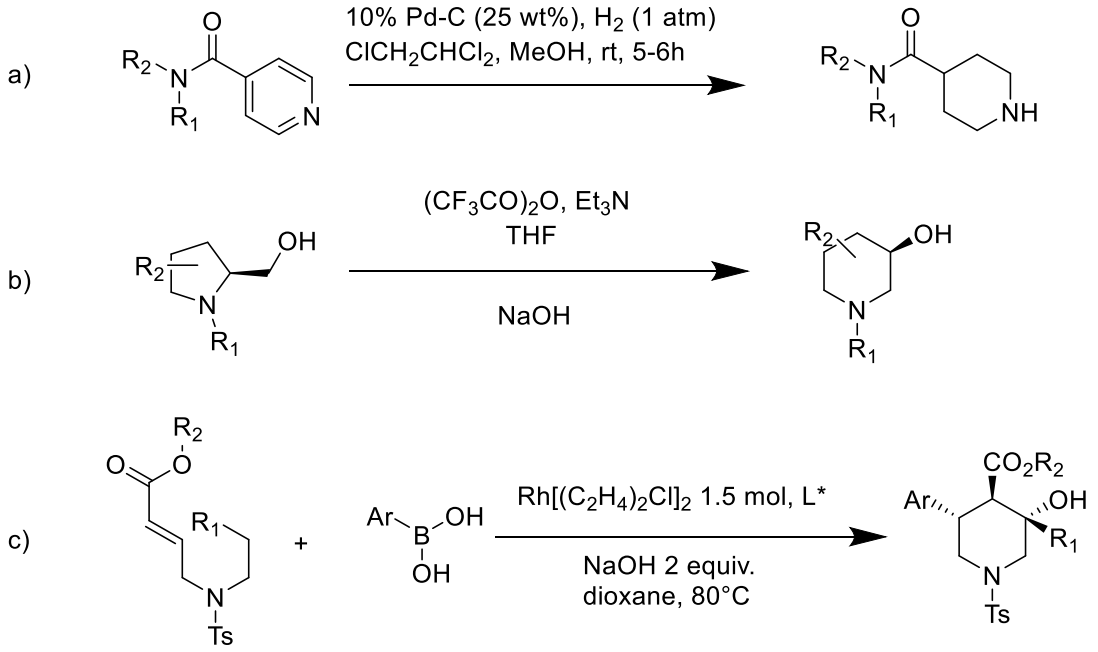

Scheme 1- Synthetic procedures for obtaining piperidine derivatives.

1.2- Morpholines

Morpholines or tetrahydro-1,4-oxazine are heterocyclic compounds in which there are two heteroatoms, a nitrogen and one oxygen, respectively in positions 1 and 4. As in the case of piperidines, morpholines have an interesting spectrum of derivatives with biological activities. These molecules are applied in many fields of pharmacology.[8] In Figure 3 are shown some examples: molecule A is morpholine; molecule B is an antidepressant agent as a selective inhibitor of the norepinephrine reuptake (NRI); molecule C is Linezolid, an antibiotic in the family of oxazolines. molecule D is a morpholine analog of doxorubicin[9], which according to some studies seems to have an anti-tumor activity 100-1000 times higher than the doxorubicin.

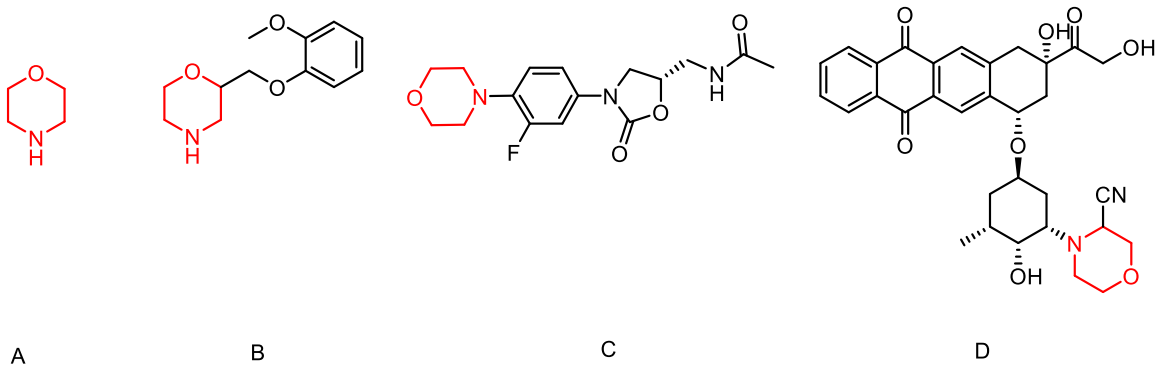

Figure 3- Example of morpholine derivatives

Again, the presence of many chiral centers requires a carefully evaluated synthetic strategy to obtain the product with the desired stereochemistry. Several synthetic methodologies are reported in the literature, the most recent and interesting are shown in Schemes 2-3. Leathen et al.[10] used a carboammination reaction catalyzed by Pd(0) to obtain cis-3,5-biofunctionalized morpholines (Scheme 2).

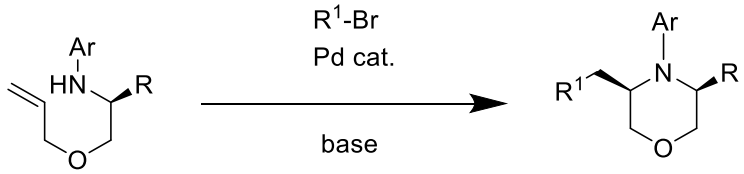

Scheme 2- Leathen synthetic procedures for obtaining morpholine derivatives.

Luescher[11] discovered a way to transform the Sn Amine Protocol (SnAP) reagents for obtaining morpholines replaced by aldehydes (Scheme 3a). Another synthetic route was reported by Fatima[12] which obtained 2,5- and 2,6- bifunctionalizated morpholines through a reaction of amino-oxygenation of alkenes (Scheme 3b).

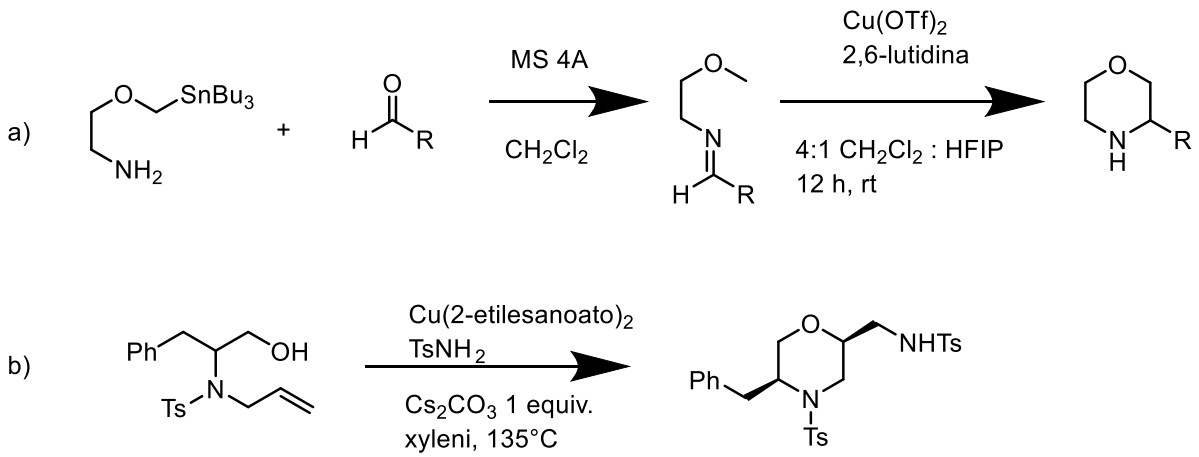

Scheme 3- Other synthetic procedures for obtaining morpholine derivatives.

2 Aim of thesis

The research team of Bernardi and coworkers[13] has developed a new synthetic strategy for obtaining substituted piperidines and morpholines with high disastereo- and enantio-selection. The reaction pathway depends on the type of nucleophile used. The result will be an intermediate and a different product as it changes the chemoselection of the nucleophile on the reaction substrate. This thesis aim is to justify the experimental outcomes through computational simulations with focus in the evaluation of transition states that lead to the main product of reaction with its stereochemistry.

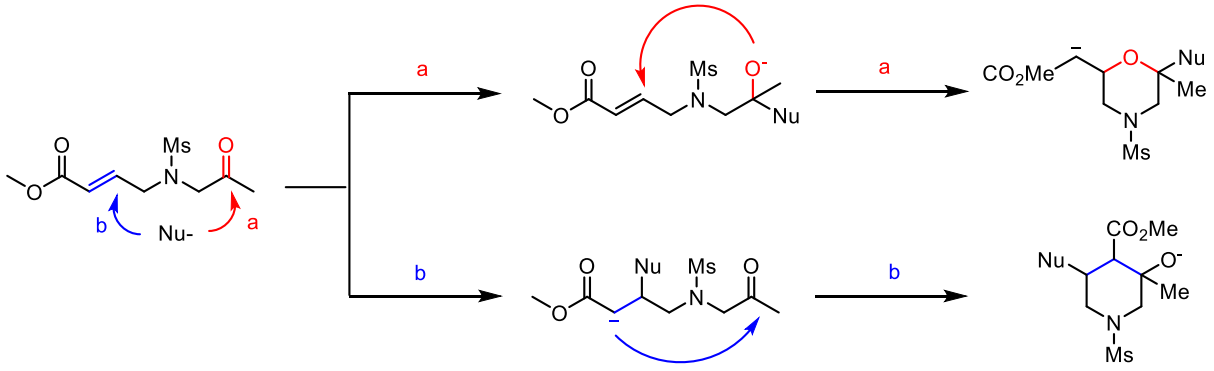

Scheme 4-Possible pathways for the nucleophile-substrate reaction.

The versatile nature of doubly electrophilic substrates, showing both a Michael acceptor, an α,β-unsaturated ester and a ketone, tethered by a heteroatom, enables two different reaction pathways. The nucleophile dictates the chemoselectivity of the reaction. Sulfa-Michael/aldol and cyanide addition/oxa-Michael results in the formation of two different classes of saturated heterocycles. The cyanide ion reaction with substrate yielded morpholine as a single diastereoisomer, with 2R*,6S* relative configuration. The phenyl-sulfide nucleophile reaction with the substrate yielded piperidine. The NMR analysis allows us to assign the 3R*,4R*,5R* relative configuration to the major diastereoisomer of the piperidine product and the 3R*,4S*,5S* to the minor one. Scheme 4 shows the two possible pathways in which the reaction may occur, the diasteroselection of reaction will be better treated in the following paragraphs.

3 Computational evaluation of reaction mechanism

The study of the reaction mechanism starts from the evaluation of the isolated reagents energies. The substrate has a high number of possible conformations being high, so it is necessary to perform a conformational analysis with a Molecular Mechanics program.

3.1- Conformational Analysis-Molecular Mechanics

In the case of organic molecules with many carbon atoms and heteroatoms within the chain, it is not easy to estimate what is the minor energy conformation for the system. Thanks to molecular mechanics (MM) algorithms, the entire conformational space of the molecule can be evaluated within a reasonable computational time. Molecular Mechanics algorithms use Force Field[14] in which angles, dihedral angles and bonding distances are reported for a wide range of chemical bonds, and the system's energy is evaluated without using quantum theory. The total energy of the system is given by the sum of many terms on interaction: energy of stretching, bending, twisting, interaction stretching-bending, interaction stretching-torsion, interaction bend-bend, non-bonding and electrostatic (charge-charge, charge-dipole, dipole-dipole):

$$U = U_s + U_b + U_t + U_{sb} + U_{st} + U_{bb} + U_{nb} + U_{el} \quad (1)$$

The stretch energy $U_s = \sum_{[bond]} U_s(i)$ is a sum over all bonds i. The single term for the bond i is:

$$U_s(i) = k_s(i) s_0 \Delta^2 l(i) [1 + s_1 \Delta l(i) + s_2 \Delta^2 l(i)] \quad (2)$$

where $\Delta l(i) = l(i) - l_0(i)$ is the deviation from the "*natural*" bond length $l_0(i)$, and $\Delta^2 l(i) = [\Delta l(i)]^2$, and s_0, s_1 and s_2 are constant. The bending energy $U_t = \sum_{[bend]} U_b(j)$ is a sum over all bendings j. The single term is

$$U_b(j) = k_b(j) b_0 \Delta^2 \theta(j) [1 + b_1 \Delta\theta(j) + b_2 \Delta^2\theta(j) + b_3 \Delta^3\theta(j) + b_4 \Delta^4\theta(j) \quad (3)$$

where $\Delta l(j) = \theta(j) - \theta_0(j)$ is the deviation from the natural bending angle between two consecutive bonds, b_0, b_1, b_2, b_3, b_4 are constants of Force Field. The torsion energy $U_t = \sum_{[torsion]} U_t(k)$ is a sum over all torsions k. The single term is

$$2U_t(k) = V_1(k)[1 + cos\phi(k)] + V_2(k)[1 - cos2\phi(k)] + V_3(k)[1 + cos3\phi(k)] \quad (4)$$

Where the dihedral angle $\phi(k)$ defines the torsion of three consecutive bonds. The mixed stretch bend energy term $U_{sb} = \sum_{[bend]} U_{sb}(j)$ gives the contribution due to a coupled stretch and bend deformation

$$U_{sb}(j) = k_{ab}(j)s_b[\Delta l(i) + \Delta l(i')]\Delta\theta(j) \quad (5)$$

where i and i' are the adjacent bonds defining the bond angle $\theta(j)$ and s_b is a constant. The mixed stretch torsion energy term $U_{st} = \sum_{[torsion]} U_{st}(k)$ gives the contribution due to a coupled stretch and torsion deformation

$$2U_{st}(k) = k_{st}(k)s_{\phi}\Delta l(i)[1 + cos3\phi(k)] \quad (6)$$

where $\phi(k)$ is the dihedral angle between three consecutive bonds and s_{ϕ} is a constant. The mixed bend-bend energy term $U_{bb}(jj') = \sum'_{[bend]} U_{bb}(jj')$ gives the contribution due to coupled bending relative to the same central atom

$$U_{bb}(jj') = k_{bb}(jj')b_b\Delta\theta(j)\Delta\theta(j') \quad (7)$$

with $k_{bb}(jj'), b_b$ constant notes in the Force-Field. The nonbonding energy term $U_{nb} = \sum_{[nb\ pairs]} U_{nb}(ab)$ gives the contribution due to the dispersion interactions of non-bonded atoms a e b :

$$U_{nb} = \varepsilon_{ab}\left[c_1 exp\left(-c_2\frac{r_{ab}}{r^*_{ab}}\right) - c_3\left(\frac{r^*_{ab}}{r_{ab}}\right)\right] \quad (8)$$

c_1, c_2, c_3, are constants r^*_{ab} is the distance relative to the maximum interaction, r_{ab} is the distance of equilibrium between two atoms and ε_{ab} is the energy of interaction between the two atoms a e b.

Once the geometries and their energies at the MM3 level are obtained, they are optimized using DFT calculations to assess what are the conformations of less energy.

3.2-Activated complex theory: actual reaction trend

Isolated reagents have usually greater energy than when they are close to the reaction distances. This is an artifice of the calculation. It can be physically explained by Van Der Waals forces, thus stabilizing reagents concerning the case of isolated reagents.[15] This consideration leads to the formulation of the theory of the activated complex (or ion-dipole complex) that is formed before the reaction for distances of some Ángström between the two reagents (see Figure 4). A similar consideration can be also made for the products, after reaction they are at a distance small enough to interact and stabilize. By removing the

products, the energy of the system increases because of Van der Waals's lack of attractive contribution. The magnitude of this force depends on the charge of the system and the distance and orientation between molecular charges and dipoles:

$$U_{vdW} = -\left[\frac{1}{(4\pi\varepsilon_0)^2 D^6}\right]\left\{\left[\frac{3\alpha_1\alpha_2 h\nu_1\nu_2}{2(\nu_1+\nu_2)}\right] + \left[\frac{\mu_1^2\mu_2^2}{3kT}\right] + [\mu_1^2\alpha_2 + \mu_2^2\alpha_1]\right\} \quad (9)$$

where the first energy term is due to the dispersive forces of London, the second to Keesom's orientation forces and the third term are Debye's inductive forces. ν_i is the rate of the fluctuation of the electronic cloud of the $i-th$ molecule, μ_i is its dipole and α_i its polarizability. As evidenced by the dependence of energy on D^{-6}, this stabilizing energy contribution is evident only for small distances and decreases rapidly. It is also evident that for polar or polarizing molecules stabilization is greater than in the case of neutral systems.

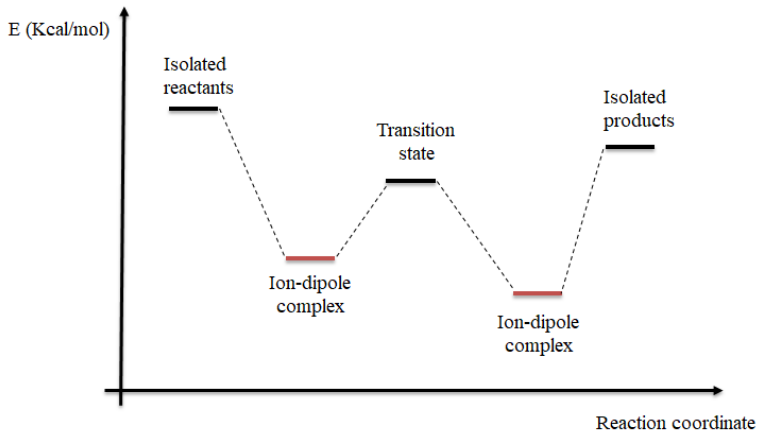

Figure 4- Activated complex (ion-dipole complex) for reactants and products.

3.3 Density Functional Theory (DFT)

The premise behind the Density Functional Theory (DFT) is that the energy of a molecule can be determined from the electron density instead of a wave function. The electronic density[16] integrated into space provides the total N number of electrons:

$$N = \int \rho(\boldsymbol{r})\,dr \quad (10)$$

since the nuclei are punctual charges, their positions correspond to local maximums of the density itself:

$$\left(\frac{\partial \overline{\rho_A}}{\partial r_A}\right)_{r_A=0} = -2Z_A\rho(\boldsymbol{r}_A) \tag{11}$$

where $\rho(\boldsymbol{r}_A)$ is the electronic density, Z_A the atomic number of atom A and $\boldsymbol{r}_A$ the radial distance of nucleus A. Before proceeding with the treatment, we need to define the term *functional*. A mathematical function is one that relates a scalar quantity to another scalar quantity, that is, $y = f(x)$. A mathematical functional relates a function to a scalar quantity and is denoted with brackets, that is, $y = F[f(x)]$. The function $\rho(\boldsymbol{r})$ depends on the spatial coordinates, and the energy depends on the values (is a functional) of $\rho(\boldsymbol{r})$. To solve it regarding the energy by DFT method, Kohn and Sham[17] proposed that the functional has the form:

$$E[\rho(\boldsymbol{r})] = T_{ni}[\rho(\boldsymbol{r})] + V_{ne}[\rho(\boldsymbol{r})] + V_{ee}[\rho(\boldsymbol{r})] + E_{xc}[\rho(\boldsymbol{r})], \tag{12}$$

where V_{ne}, the nuclear-electron attraction term is

$$V_{ne}[\rho(\boldsymbol{r})] = -\sum_{K}^{nuclei} \int \frac{Z_K}{|\boldsymbol{r} - \boldsymbol{r}_K|}\rho(\boldsymbol{r})d\boldsymbol{r}\,, \tag{13}$$

and $V_{ee}[\rho(\boldsymbol{r})]$, the classical electron-electron repulsion term is:

$$V_{ee}[\rho(\boldsymbol{r})] = \frac{1}{2}\int\int \frac{\rho(\boldsymbol{r}_1)\rho(\boldsymbol{r}_2)}{|\boldsymbol{r}_1 - \boldsymbol{r}_2|} d\boldsymbol{r}_1 d\boldsymbol{r}_2 \tag{14}$$

The real key, however, is the definition of the first term of Eq 12. Kohn and Sham defined it as the kinetic energy of noninteracting electrons whose density is the same as the density of the true interacting electrons. The last term, $E_{xc}[\rho(\boldsymbol{r})]$, is the so-called exchange-correlation energy and is a catch-all term to account for all other aspects of the true system. The operator corresponding to the expression of energy shown in Eq 12 is the so-called single-electronic operator of Kohn-Sham (KS):

$$\hat{h}_i^{KS} = -\frac{1}{2}\nabla_i^2 - \sum_K \frac{Z_K}{|\boldsymbol{r}_i - \boldsymbol{r}_K|} + \int \frac{\rho(\boldsymbol{r}')}{|\boldsymbol{r}_i - \boldsymbol{r}'|} d\boldsymbol{r}' + \hat{V}_{xc} \tag{15}$$

The Kohn-Sham procedure is then to solve the equation that minimizes the energy, which reduces to the set of pseudoeigenvalue equations (in Figure 5 an example of a self-consistent strategy for geometry optimization):

$$\sum_{i=1}^{N} \hat{h}_i^{KS} |\chi_1 \chi_2 \cdots \chi_N\rangle = \sum_{i=1}^{N} \varepsilon_i |\chi_1 \chi_2 \cdots \chi_N\rangle. \quad (16)$$

The Hoenmberg-Kohn Theorem proves the existence of a functional that relates the electron density to the energy, but it doesn't explain the form of that functional. The real problem is the exchange-correlation (E_{xc}) term of the equation. There is no way of deriving these terms, and so a series of different functionals have been proposed, leading to dozens of different DFT methods. The functional exchange-correlation can be expressed through an interaction between electronic density ρ and energy density ε_{xc}. The second term can also be written as the sum of two contributions, the exchange ε_x, and the correlation ε_c . The impossibility of formulating an expression for the two functionals has led to the introduction of approximations, the most used is the "*Local Density Approximation"* (LDA). In this model, the value of ε_{xc} depends only on the "local" value of ρ. The only condition necessary to establish the value of the exchange-correlation functional at a given r coordinate is that it has a unique value for this coordinate. This approximation is valid for some systems such as a uniform electron gas, but not too exhaustive for a system of chemical interest. One solution to improve the model is to consider ε_{xc} dependent on the local value ρ and the charge density local variation. This essentially means including the dependence on the density gradient. The functionals are called "gradient-correct" and the corresponding approximation is called "generalized gradient approximation" (GGA). The GGA-functionals are usually built from the LDA functional by inserting a corrective term.

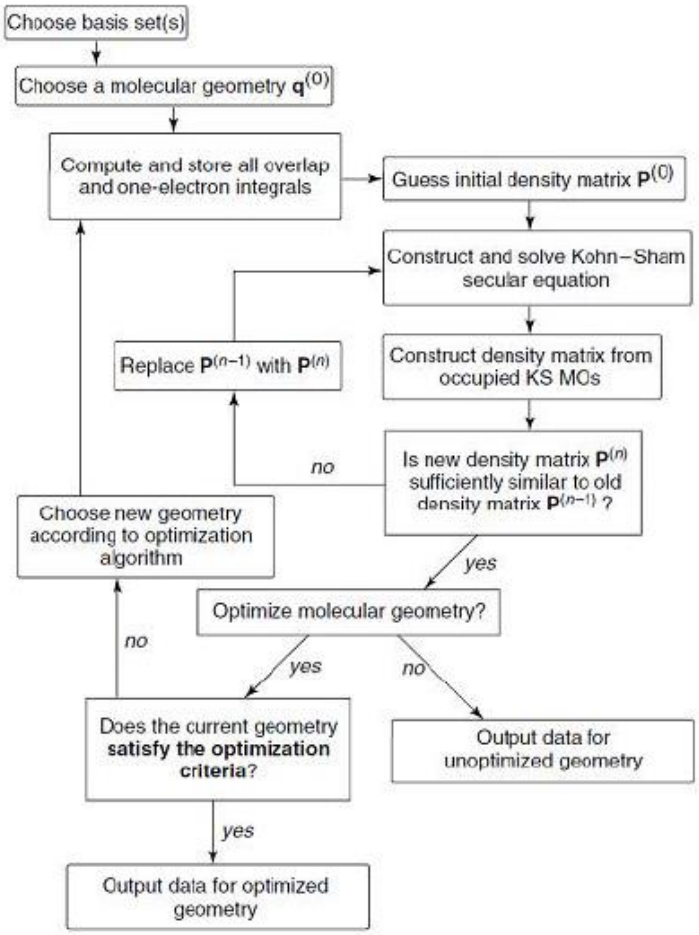

Figure 5-Self-consistent procedure for DFT geometry optimization.

3.3.1 Functional classification

As introduced in the previous paragraph, the first classification of density functionals is between local and non-local functionals[16]. "Local" functionals can then be divided into other categories:

1) LSDA Functional: Only consider the local spin density
2) GGA functional: they depend not only on the local spin density but also on the gradient near the position of the charges themselves,
3) Meta-GGA functional: in addition to the value of the local spin density, the energy of exchange also depends on the density of kinetic energy of exchange.

Non-local functionals are in turn constructed by the local ones by evaluating the exchange and correlation energy components also with Hartree-Fock theory. Through typical formulas for each functional is then made a weighted average of the two estimations of exchange and

correlation energy. For example, if the exchange energy of a GGA or meta-GGA is evaluated as the average between DFT theory and HF you get a Hybrid-GGA and a hybrid meta-GGA functionals respectively. However, there are also functionals in which the energy component of exchange and correlation is fully evaluated at the HF level.

3.3.2 B3LYP functional

Among the most popular GGA exchange functionals, there is the one developed by Becke. In the acronym that identifies the functional is simply indicated with B. For the correlation functionals, the most used is the one indicated by the acronym LYP (Lee-Yang-Parr). If the Becke Exchange Functional is paired with the correlation functional Lee-Yang-Parr the resulting DFT method is named BLYP. The B3LYP exchange energy can be expressed in terms of Hartree-Fock's contribution E_x^{HF} and DFT exchange energy DFT, E_x^{LSDA}:

$$E_x = (1-a)E_x^{LSDA} + aE_x^{HF} \tag{17}$$

It is possible to use one or more parameters in the expression. In the case of the B3LYP[18] method, widely used in this thesis, the empiric parameters are 3:

$$E_{xc}^{B3LYP} = (1-a)E_x^{LSDA} + aE_x^{HF} + b\Delta E_x^{HF} + (1-c)E_c^{LDA} + cE_c^{LYP} \tag{18}$$

where the optimized parameters turn out to be a=0,20, b=0,72 and c=0,81. This functional use Becke's exchange functional, the correlation functional of Lee-Yang-Parr and 3 empiric parameters.

3.3.3 M06-2X functional

The functional M06-2X[19] is a hybrid meta-GGA functional with a high "non-locality" in assessing energy terms of electronic exchange. This functional is very high performing compared to others in estimating the energy of systems in which the dispersion, induction and non-covalent forces are the main contributors in assessing the energy of the system of interest. In the M06-2X algorithm, the local part of the electronic density is a function of 3 variables: the local spin density ρ_σ, the reduced gradient of the spin density χ_σ and the spin kinetic energy density τ_σ:

$$\chi_\sigma = \frac{|\nabla\rho_\sigma|}{\rho_\sigma^{4/3}} \tag{19}$$

$$\tau_\sigma = \frac{1}{2}\sum_{i}^{occup} |\nabla\psi_{i\sigma}|^2 \tag{20}$$

with $\sigma = \alpha,\beta$ spin states relative to the arbitrary axis of the electron's angular spin moment. Energy's dependence on the kinetic energy density of spin in the algorithm allows for a better representation of the London and Debye forces of the molecular system. These forces depend on the polarization of the molecule and the speed of electrons around the nuclei. For this reason, a better description of the kinetic contribution allows a better evaluation of these forces. In the case of the functional M06-2X, the energy exchange-correlation contribution is expressed as:

$$E_{XC}^{hyb} = \frac{X}{100}E_X^{HF} + \left(1 - \frac{X}{100}\right)E_X^{DFT} + E_C^{DFT} \tag{21}$$

where E_X^{HF} is the Hartree-Fock (HF) non-local exchange energy, X is the percentage of Hartree-Fock energy in the hybrid functional, E_X^{DFT} is the local exchange energy evaluated at the DFT level and $E_C^{DFT}$is the local correlation energy calculated at the DFT level. X is evaluated through working functions and the percentage chosen is the one that ensures self-consistency in the solution of Kohn-Sham equations.

3.3.4-Basis set

Basis set functions are mathematical functions that are used to construct the wave function of the system being examined using the LCAO (linear combination of atomic orbitals) method. The basis functions most used today for quantum-mechanical calculations are GTO (Gaussian Type Orbital) functions that in Cartesian coordinates have the following form:

$$\varphi(x,y,z,\alpha,i,j,k) = \left(\frac{2\alpha}{\pi}\right)^{3/4}\left[\frac{(8\alpha)^{i+j+k}\,i!\,j!\,k!}{(2i)!\,(2j)!\,(2k)!}\right]x^i y^j z^k e^{-\alpha(x^2+y^2+z^2)} \tag{22}$$

where α is the exponent that controls the width of the gaussian, while i,j,k are integers (positive) that specify the nature of the orbital. For example, if i,j,k are zero, the corresponding GTO has spherical symmetry and is, therefore, a GTO of type s. If one of the three indices is equal to one and the other two are zero, the GTO is of type p. A huge advantage in using Gaussians as basis functions is that the product of two Gaussians with different centers is equal to a Gaussian with a center along the connecting line of the two centers. This mathematical characteristic allows the analytical solution of the integrals to 4

indices due to the coulombian and exchange operators. The GTOs, however, are characterized by a radial trend of the type e^{-r^2} which does not describe well the shape of the wave functions of the hydrogenoid orbitals to tend to zero and to tend to infinity of the distance r from the core. For these reasons, linear combinations of GTO are preferred:

$$\varphi(x,y,z,\{\alpha\},i,j,k) = \sum_{a=1}^{M} c_a \varphi(x,y,z;\alpha_a,i,j,k) \tag{23}$$

where M is the number of Gaussian functions used in the combination and the coefficients c_a are chosen to optimize the performance of the function and ensure its normalization. Basis functions constructed as a combination of Gaussian functions are referred to as "contracted" basis function, while Gaussian functions that are combined to form the base are called "primitives". The contraction can be of two types:

- Segmented: a set of different GTOs primitive functions are used to generate different contracted functions.
- General: a single set of primitive functions is used to generate multiple contracted functions.

General contraction is less expensive than segmented one, the first type of contraction significantly reduces the number of bicentric and overlapping integrals. It is necessary to briefly introduce the nomenclature that characterizes the basis set used in this work. Two bases set type were used:

- 6-31G(d), with a B3LYP functional;
- 6-311+G(d), with an M06-2X functional.

These two basis sets are "split-valence" and were developed by Pople and collaborators.[20] For instance, in the 6-31G(d) acronym, the number 6 before the ident indicates the number of primitives used to generate the only contracted function to describe the core orbitals. The number after ident indicates the number of primitive functions used to generate contracted functions to describe valence orbitals. If after the ident there are 2 numbers, it means that 2 functions are generated for the valence orbitals, so it is a base of type "double-zeta". If there are 3 numbers after the ident, 3 functions are generated to describe the valence orbitals and are, therefore, a "triple-zeta" base. In the 6-311+G(d) basis set, three primitive functions are used to generate a contracted function of valence while the other two primitive functions are used uncontracted. The plus in the basis set acronym indicates the presence of diffuse

functions. These functions are used to make a base more flexible and well-described electrons that are in a region far from maximum electronic density. These are “loose” functions, Gaussian functions with very small exponents, and therefore are radial spread.

3.4- Comparison of ab-initiio methods and DFT methods

Hybrid functionals are the most efficient whit average errors comparable to those of multilevel related methods, but with much larger maximum errors. In many cases, the accuracy of DFT methods is due to a cancellation of error. An increase in the size of the base generally does not lead to an improvement in the result. Literature shows that the B3LYP/6-31G(d) combination performs very well not only in energy but also in the optimization of geometries and the calculation of molecular proprieties. In the B3LYP theory, energy is a function of the local density and at most of the gradient of the same. The functional B3LYP is not able to describe the dispersive forces and therefore is not able, without empiric corrections, to describe all those systems in which dispersive forces are fundamental, such as Van der Waals systems. Another problem with DFT methods is that it is difficult to accurately describe excited systems. In the case of *ab-initio* methods, it is easy to describe excited electronic states as they arise from the promotion of electrons in unoccupied orbitals, which is not possible for DFT methods.

3.5-Potential energy surface (PES)

Within the Born-Oppenheimer approximation, it is possible to define, for a given molecular system, a surface of potential energy (PES). It describes molecular energy according to the positions of nuclei: it is a hypersurface function of the 3N-6 internal coordinates that describe the structure of the molecule (where N is the number of atoms). From the structure of the PES, it is possible to determine various information such as molecular structure, rotational or vibrational spectrum, kinetic and dynamics of nuclear motion and mechanism of the reaction. The mechanism of a reaction can be analyzed by the evaluation of the reactive system PES. In the study of molecular PES, the points of greatest chemical interest are the stationary points. Those points are the ones in which the gradient of molecular energy, relative to all internal coordinates, cancels out. The analysis of the Hessian matrix allows determining what type of stationary point is being analyzed. For example, a minimum point is characterized only by positive second derivatives, a point of maximum vice versa has only negative second-derived. A given geometry of the molecular system in which only one term is negative in the hessian matrix and the remaining positives is mathematically defined as a saddle point. In the case of

a reactive system, it corresponds to the transition state of the reaction considered. Once the energies at a set of chosen nuclear geometries are calculated, they must be evaluated with an analytical expression that allows us to describe the portion of PES mapped in its entirety. Also in the case of a large molecular system, it is possible to make a mapping of the portion of PES analyzed. This is done according to a selected set of internal coordinates such as an intermolecular distance or a torsional coordinate.

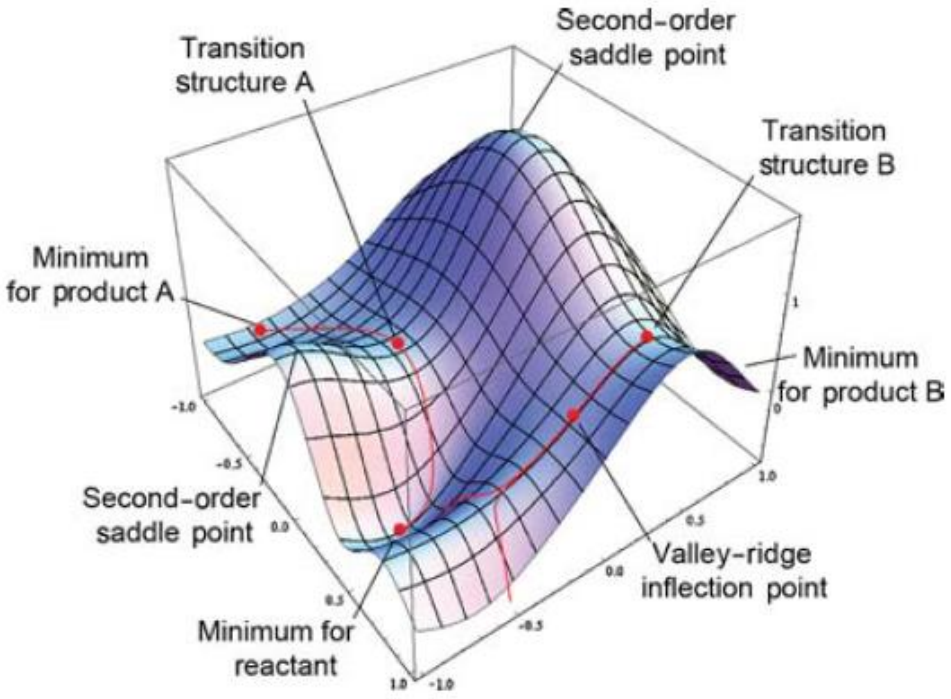

Figure 6- Molecular PES with stationary point example

3.7- IRC- Internal Reaction Coordinate evaluation of the reaction mechanism

The absolute rate theory of Eyring,[21] which provided a useful theoretical tool for studying chemical reactions, is essentially associated with the concept of "transition state", a unique state on the potential energy surface of the reacting system. The evaluation of the absolute rate of reaction involves the following steps:

1- Calculate the potential energy function in terms of the atomic positions;
2- Obtain the transitions state, reactant and product points;

3- Determine unequivocally the reaction path connecting the relevant stable points and the transition state point;
4- Calculate the absolute rate of the nuclear rearrangement along the reaction path by appropriate quantum statistical mechanical approaches.

Ab initio quantum-chemical methods allow to calculate the total energy of a molecular system with a fixed nuclear arrangement-adiabatic potential (V), based on the Born-Oppenheimer approximation. We represent the nuclear configuration of a chemically reacting system composed of N nuclei by a point in 3N-dimensional configuration space with space-fixed 3N Cartesian coordinates, $X_\alpha, Y_\alpha, Z_\alpha \quad (\alpha = 1,2,\dots,N)$. The potential energy function V can be represented in term of $X_\alpha, Y_\alpha, Z_\alpha$, and we can obtain the equilibrium points as satisfying:

$$\frac{\partial V}{\partial X_\alpha} = \frac{\partial V}{\partial Y_\alpha} = \frac{\partial V}{\partial Z_\alpha} = 0 \qquad \alpha = (1,2,\dots,N) \tag{25}$$

The molecules react to each other by vibrating from an equilibrium configuration, possibly rotating around the center of mass and exchanging energy against all degrees of freedom. The IRC[22] Internal Rate Coordinate approach allows to connect reagents, transition state, and products and is based on the classic motion equation:

$$\frac{d}{dt}\left(M_\alpha, \dot{X}_\alpha\right) = -\frac{dV}{dX_\alpha} \quad etc. \tag{26}$$

Considering a movement from a point of equilibrium to an infinitesimal velocity:

$$M_\alpha \dot{X}_\alpha = -\frac{dV}{dX_\alpha} t + costant, etc. \tag{27}$$

By assumption, the nuclear motion takes place with an infinitesimal velocity, at the time $t = 0, \dot{X}_\alpha = 0$ the integration constant is zero and you get:

$$\dots = \frac{M_\alpha dX_\alpha}{\frac{\partial V}{\partial X_\alpha}} = \frac{M_\alpha dY_\alpha}{\frac{\partial V}{\partial Y_\alpha}} = \frac{M_\alpha dZ_\alpha}{\frac{\partial V}{\partial Z_\alpha}} = \cdots \tag{28}$$

Adopting the mass-weighted Cartesian coordinates in which:

$$M_\alpha^{1/2} X_\alpha = x_{3\alpha-2}\,, \qquad M_\alpha^{1/2} Y_\alpha = x_{3\alpha-1}\,, \qquad M_\alpha^{1/2} Z_\alpha = x_{3\alpha}\,, \tag{29}$$

with the kinetic energy expression:

$$T = \frac{1}{2}\sum_{i=1}^{3N} \dot{x}_i^2 \tag{30}$$

The use of 3N Cartesian coordinates is not suitable for discussing the potential energy surface since these coordinates include translational and rotational motion. Thus, it is worthwhile to reduce the number of variables to 3N–6 by eliminating the translation and the rotation of the reacting system. It's easy to get the connection between Cartesian coordinates and the internal coordinates of the reactive system.

$$dq_i = \sum_{\alpha=1}^{N} \left(\frac{\partial q_i}{\partial X_\alpha} dX_\alpha + \frac{\partial q_i}{\partial Y_\alpha} dY_\alpha + \frac{\partial q_i}{\partial Z_\alpha} dZ_\alpha \right) \tag{31}$$

with $i = (1,2, \dots, N)$, adding the following six relations:

$$\sum_\alpha M_\alpha dX_\alpha = \sum_\alpha M_\alpha dY_\alpha = \sum_\alpha M_\alpha dZ_\alpha = 0 \tag{32}$$

$$\sum_\alpha M_\alpha (Y_\alpha dZ_\alpha - Z_\alpha dY_\alpha) = \sum_\alpha M_\alpha (Z_\alpha dX_\alpha - X_\alpha dZ_\alpha) = \sum_\alpha M_\alpha (X_\alpha dY_\alpha - Y_\alpha dX_\alpha) = 0 \tag{33}$$

Which assures a zero total momentum and zero total angular momentum motion. Then, we get 3N linear simultaneous equation for 3N unknowns $dX_\alpha, dY_\alpha, dZ_\alpha$ from which we obtain:

$$dX_\alpha = \sum_{i=1}^{n} \frac{\partial X_\alpha}{\partial q_i} dqi\,, \quad dY_\alpha = \sum_{i=1}^{n} \frac{\partial Y_\alpha}{\partial q_i} dqi\,, \quad dZ_\alpha = \sum_{i=1}^{n} \frac{\partial Z_\alpha}{\partial q_i} dqi, \tag{34}$$

Putting these relations into the kinetic energy formula in eq 30, the result is:

$$T = \frac{1}{2}\sum_{i,j=1}^{n} a_{ij}\dot{q}_i\dot{q}_j \tag{35}$$

in which

$$a_{ij} = \sum_{\alpha=1}^{N} M_\alpha \left(\frac{\partial X_\alpha}{\partial q_i}\frac{\partial X_\alpha}{\partial q_j} + \frac{\partial Y_\alpha}{\partial q_i}\frac{\partial Y_\alpha}{\partial q_j} + \frac{\partial Z_\alpha}{\partial q_i}\frac{\partial Z_\alpha}{\partial q_j} \right) \tag{36}$$

These matrix elements are hard to obtain, and what is usually do is get the elements of the reverse matrix:

$$a_{ij}^{-1} = \sum_{\alpha=1}^{N} M_\alpha{}^{-1}\left(\frac{\partial q_i}{\partial X_\alpha}\frac{\partial q_j}{\partial X_\alpha} + \frac{\partial q_i}{\partial Y_\alpha}\frac{\partial q_j}{\partial Y_\alpha} + \frac{\partial q_i}{\partial Z_\alpha}\frac{\partial q_j}{\partial Z_\alpha}\right) \tag{37}$$

and then from these get the terms of the a_{ij} matrix. To better visualize the structure of IRC calculation in a chemical way it is possible to refer to an internal coordinate system called the internal-F coordinate (see Figure 7). If we refer to a certain intramolecular distance between two nuclei a e b (Rab) we can relate it to the various coordinates q_i:

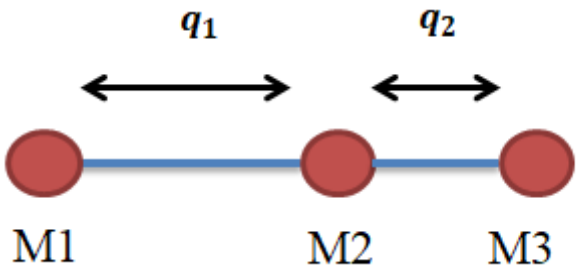

Figure 7- Example of normal coordinate involved in the formation/dissociation of a chemical bond.

Where M1, M2, and M3 are the masses of three atoms in the reagent system. q_1 and q_2 are the normal vibration coordinates involved in the dissociation or association mechanism of atoms in the system. Once obtained a classical formulation for a physical quantity is possible to translate this formulation into an operator, apply it to a certain wave function and get the corresponding observable after integration and normalization. Writing than the classic Hamiltonian as:

$$\mathcal{H} = \frac{1}{2}\sum_{i,j} a_{ij}^{-1} + P_i P_j + V \tag{38}$$

Where a_{ij}^{-1} is a function of normal vibration coordinates q_i and P_i is the conjugate moment to q_i. The corresponding quantum Hamiltonian operator proposed by Podolsky[23] is:

$$\mathcal{H} = \frac{1}{2}\sum_{i,j} a^{-\frac{1}{4}}\left(-i\hbar\frac{\partial}{\partial q_i}\right)a_{ij}^{-1}a^{\frac{1}{2}}\left(-i\hbar\frac{\partial}{\partial q_j}\right)a^{-1/4} + V(q_1, q_2, \ldots q_N) \tag{39}$$

In this formula $a = det(a_{ij})$. Once the energy is determined, it is graphed to the reaction coordinate. The result is a diagram that shows the fundamental states of reagents, products and the transition state that connects them. In Figure 8 is represented the evolution of the energy and the gradient of the same relative to the internal coordinate of reaction. The TS

corresponds to a maximum point concerning the reaction coordinate and therefore a saddle point whit respect to the entire PES. The fundamental states of products and reagents are instead minimal in both representations. For all three systems, the gradient cancels out because in all the three cases is checked that they are stationary points.

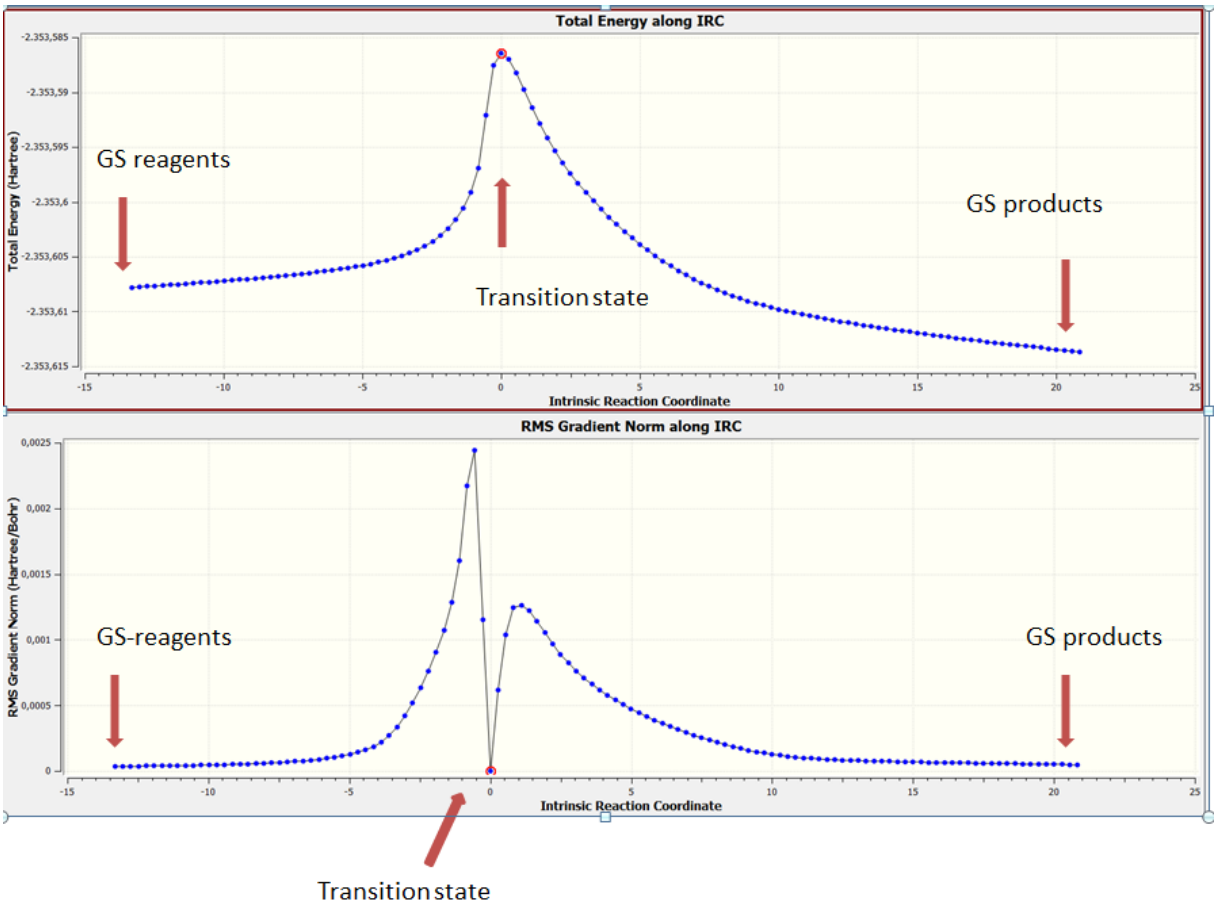

Figure 8- The graph above shows the energy trend against intrinsic reaction coordinate, at the bottom the trend of the energy gradient relative to the intrinsic coordinate of reaction.

3.7- Solvation energy- SMD approximation

Once the reagents structures, products, and transition states have been obtained, it is necessary to transport the system from the gas phase to the actual reaction environment (solvent).[24] This essentially means assessing the free energy (or similarly the enthalpy) of dissolution. The standard-state free energy of solvation, that is the standard-state free energy of transfer from the gas phase to the condensed phase, may be partitioned according to

$$\Delta G_S^\circ = \Delta G_{ENP} + G_{CDS} + \Delta G_{conc}^\circ \qquad (40)$$

Or equivalently in terms of enthalpy:

$$\Delta H_S^\circ = \Delta H_{ENP} + H_{CDS} + \Delta H_{conc}^\circ \quad (41)$$

The ENP subscript in Eq. 40 denotes the electronic (E), nuclear (N), and polarization (P) components of the free energy. The nuclear relaxation component of the ENP term is equal to the difference between the gas-phase total energy calculated at the gas-phase equilibrium structure. If the geometry is assumed to be the same in the gas phase and the liquid phase, then the ENP term becomes just an electronic polarization (EP) term. The CDS subscript in Eq. 40 emphasizes that the corresponding term is nominally associated with the free energy change due to solvent cavitation (C), changes in dispersion (D) energy, and possible changes in local solvent structure (S). The final term in Eq. 40 accounts for the concentration changes between the gas-phase standard state and the liquid-phase standard state. Since here the same concentration (1 mol/L) is used in both the gaseous and solution phases, ΔG_{conc}° is zero.

4- Computational strategy

The computational strategy used to evaluate the reaction mechanism is the same for both the nucleophiles considered. A scan approach was first performed for the nucleophile closer to the two reaction sites requiring the minimization of the energy of the system. This is equivalent to solving a problem with Lagrange multipliers. The minimization is required by imposing as a constraint the variation of the length of the bond that is forming in the reaction. The result of this calculation will be similar to the one shown in Figure 13. In the starting point of the scan, the nucleophile is placed at a distance far enough away from the electrophile site. The approach leads to an increase in energy until it reaches a local maximum compared to the chosen coordinate, which corresponds to the transition state of the system. The evidence that is a stationary point is provided by the graph below in Figure 9. It expresses the energy gradient relative to the scan coordinate and is null at the transition state. A further approach leads to the formation of the bond until it reaches its length of balance. When this distance of stability is exceeded, there is an increase in energy for the establishment of repulsive forces. The result of this scan is a geometry very close to the actual geometry of the transition state, a subsequent optimization with an algorithm implemented for TS search leads to the exact geometry. Once the TS is obtained the IRC calculation is made and the result is the structure of reagents and products related to it. The product obtained by the addition of nucleophile in the transition state is the intermediate of the full reaction analyzed. The next passage is a cyclization that leads to the formation of piperidine or morpholine cycle. It can be

reproduced starting from the intermediate. A more functional strategy, however, is to start the scan from the cyclical product and ward off the atoms that form the bond. Again, the scan proceeds with the minimization strategy mentioned above, but the resulting scan will be a mirror image of the one in Figure 9. Another difference is that the repulsive component for small distances is neglected as the scan starts from the equilibrium distance for the bond. This strategy is justifiable through the Hammond principle.[25] For a cyclization, the state of transition that leads to the formation of the cycle will be much more geometrically similar to the products compared to the reagents. A further consideration comes from the fact that the reaction is catalyzed by a quaternary ammonium salt, the position of the same within the reaction environment must be chosen carefully to simulate its catalytic effect. The position of the catalyst determines the preferred transition state in terms of chemoselectivity and diasteroselection. Finally, once the geometries of transition states, products and reagents were obtained at the B3LYP/6-31G(d) level, these are used to calculate electronic energies with a more accurate level evaluating also the solvent contribution. The choice fell on the functional M06-2X and a 6-311+G(d) basis, this level of calculation was chosen because of its predisposition to the description of the energy of reactive systems. The choice to use enthalpy instead of the Gibbs free energy was dictated by the presence of many low-energy vibrators that hamper a suitable evaluation of the entropic factor, even if the correction was applied.[26] The presence of the reaction solvent (toluene) was assessed by the SMD approximation. Since the reactions considered are under "kinetic control" or carried out with low temperatures and reaction times the major product is the one that derives from the transition state with lower energy.

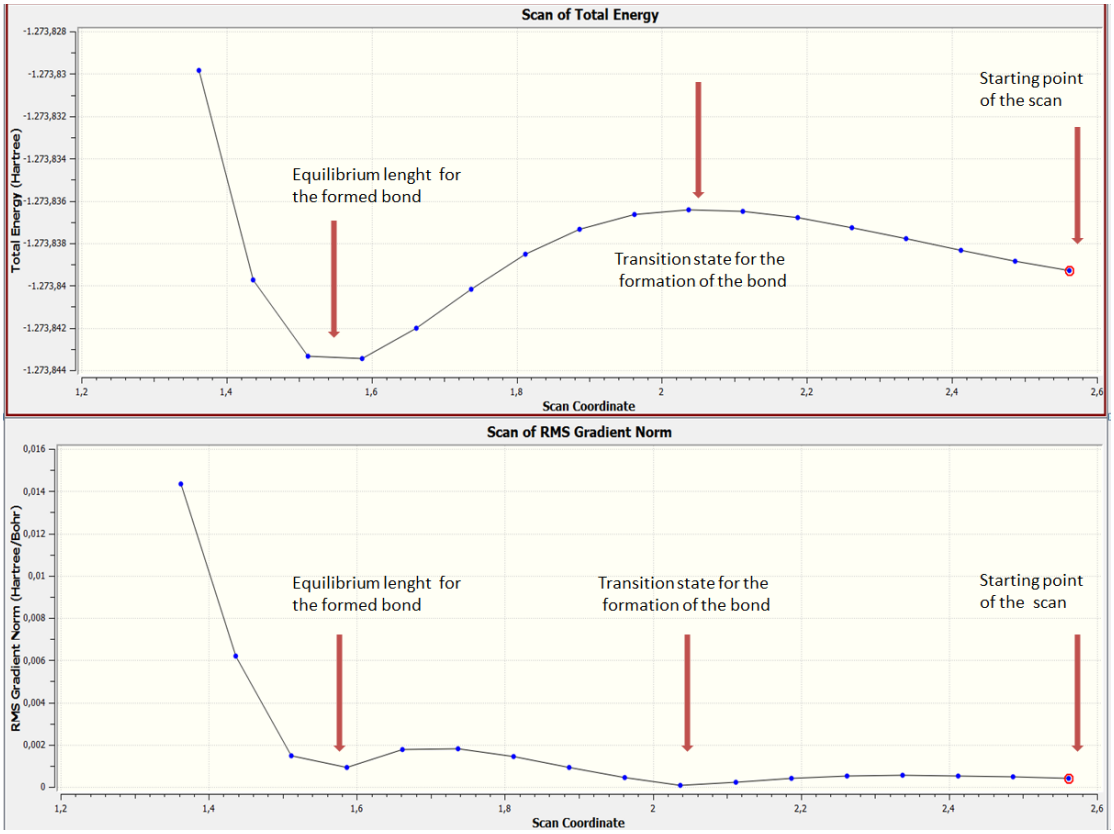

Figure 9- The energy and gradient of the energy during the formation of a bond

4.1-Reaction with cyanide

To better simulate reactions, it is necessary to know precisely the experimental conditions that led to the main product. The reaction between cyanide and substrate was carried out in the conditions shown in Scheme 5:

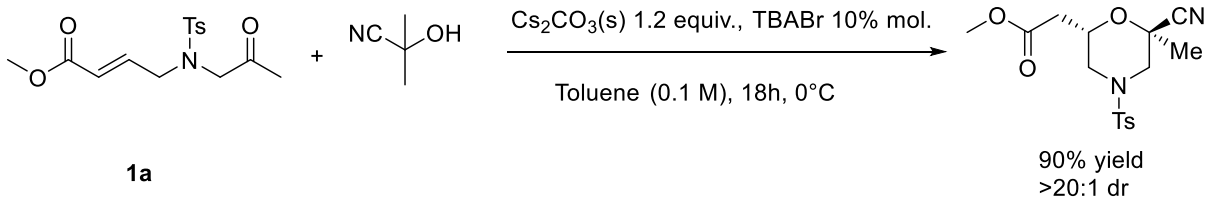

Scheme 5- Experimental conditions for the reaction between cyanide and substrate.

This is an aldol/oxa-Michael cascade reaction between substrate **1a** and cyanide ion as a nucleophile. Acetone cyanohydrin, was chosen as reagent as it generates the nucleophile *in situ* avoiding its dispersion in the environment. The mechanism behind this reaction includes the nucleophilic attack of cyanide on the ketonic site, with the formation of a first chiral center, followed by an oxa-Micheal cyclization reaction, as shown in the Scheme 6.

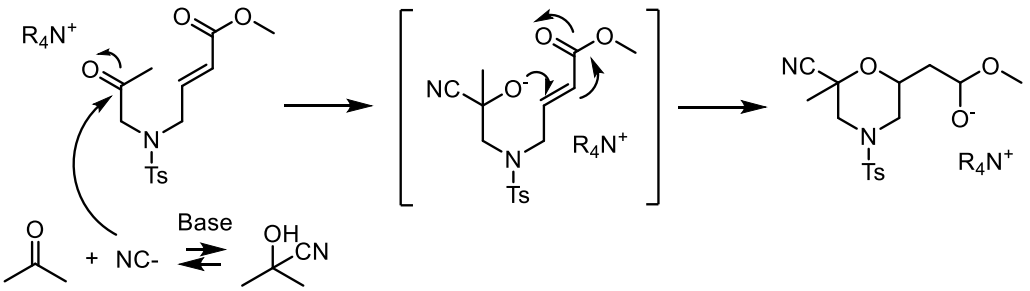

Scheme 6- The proposed mechanism for the addition of cyanide to the starting substrate.

The reaction is diastereoselective and the resulting morpholine has a 2S*, 6R* relative configuration, experimentally determined by ^{1}H-NMR NOE spectroscopy.[27] To explain the formation of a single diastereoisomer, a stereochemical pseudo-chair transition state model was proposed (Figure 10). In this transition state, the methyl and the methoxy occupy an equatorial position in order to reduce the steric clash.

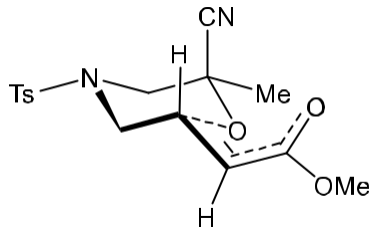

Figure 10- Chair transition state leading to majority diastereoisomer.

4.1.1 Computational details

The simulation of the reaction was carried out by making some changes to the reaction scheme to reduce the computational cost. The nitrogen-linked tosylate group, which was not involved in the reaction, was replaced by a mesyl group. The catalyst used experimentally is tetrabutylammonium bromide, that has been replaced by tetramethylammonium (TMA). These substitutions reduce significantly the computational cost and do not change the chemistry of the system. Whit this reaction model, the two transition states relative to the possible nucleophilic additions have been simulated. The transition state called TS_1^A is relative to the addition of cyanide to the ketone, while TS_1^B is relative to the addition of cyanide to the α,β-position to the ester (Figure 11). Cyanide ion was placed dissociated from cyanohydrin at a distance of about 2.5 Å from the ketonic carbonyl for the first transition state. To prove the unfeasability of the other TS, the cyanide has been placed near the double bonding in the β-position to the ester and the TS energy was evaluated in parallel to TS_1^A.

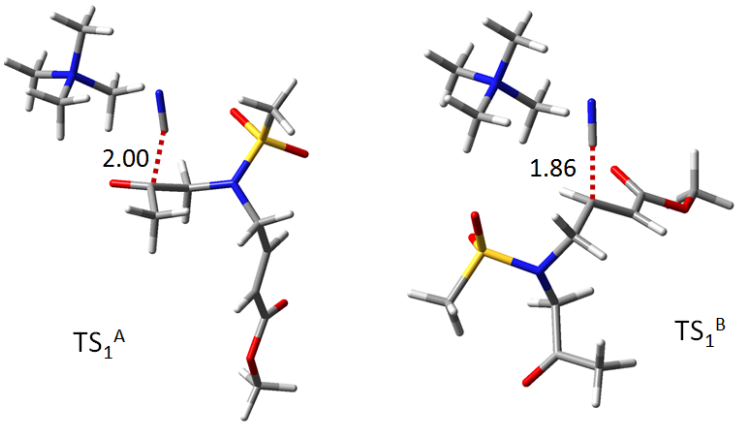

Figure 11- Representation of cyanide addition to the two possible reaction sites with distances in Å.

The presence of the catalyst is really important in these TS, because, in both cases, it is close to the reaction site. In TS_1^A the tetramethylammonium has an interaction with the oxygen of the ketonic carbonyl. Its function is to activate the carbonyl and make it more electrophile to the nucleophilic addition. In TS_1^B, the catalyst is between the ester and the conjugate α,β-unsaturated bond, probably for its interaction with the delocalized charge. Once the transition states were obtained, the IRC calculations were carried out. The two activated complexes and the two intermediates leading to their respective reaction paths were obtained. After these geometries optimization, the lowest energy one will be used as a reference level for the evaluation of the activation energy of the two reaction pathways. In this case, it is the reagents activated complex of the first TS, that is AC^A (Figure18, Scheme 7).

Table 1- Relative energies for the addition of cyanide on the two possible sites: ketone carbon (pathway A) or the α,β-unsaturated bond (pathway B).

	Opt EE (B3LYP) (a.u.)	H_corr (B3LYP) (a.u.)	SP EE (MO6-2X) (a.u)	SP+H_corr (a.u)	Rel E (Kcal/mol)
AC^A	-1488.151749	0.450066	-1488.014437	-1487.564371	0
AC^B	-1488.150941	0.449793	-1488.013469	-1487.563676	0.4
TS_1^A	-1488.131421	0.449261	-1487.996377	-1487.547116	10.8
TS_1^B	-1488.121723	0.448724	-1487.987185	-1487.538461	16.2

Int$_1^A$	-1488.146006	0.449945	-1488.009194	-1487.559246	3.2
Int$_1^B$	-1488.160677	0.450335	-1488.024988	-1487.574653	-6.5

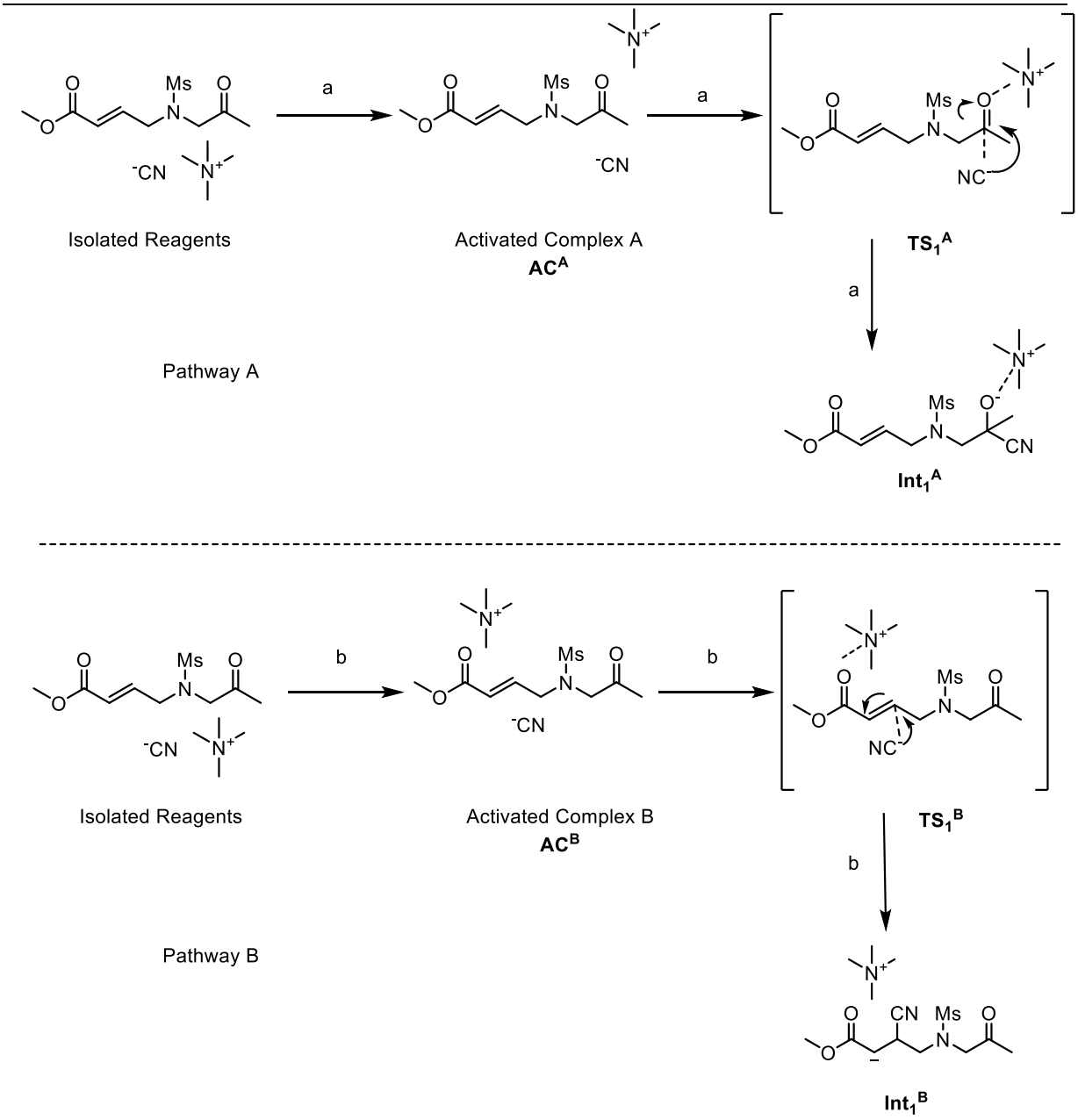

Scheme 7- Molecular species considered in Table 1.

The enthalpy is evaluated as:

$$H = EE^{M06-2X/6-311+G(d)} + H_{corr}^{0\ B3LYP/6-31G(d)} \quad (42)$$

Where $EE^{M06-2X/6-311+G(d)}$ is the electronic energy (single point) evaluated with M06-2X/6-311+G(d), while $H_{corr}^{0\ B3LYP/6-31G(d)}$ is the enthalpy correction to electronic energy evaluated at the B3LYP/6-31G(d) level of calculation. Pleasingly, the first attack of the

nucleophile on the ketone carbonyl is at an energy of 5.6 Kcal/mol lower than the attack on the β-position to the ester, according to the experimental evidence.[13, 28] The second stage of the reaction that converts **Int_1^A** to morpholine cycle and **Int_1^B** to the formation of a piperidine cycle was carried out as mentioned in the computational strategy. The energy scan started from the cyclic product and wards off the atoms that form the bond of interest. In the reaction pathway to piperidine, the catalyst is placed on the ketone-derived alkoxy, whereas for the morpholine product it is placed on the oxygen of the ester carbonyl. The two energy scans lead to obtain TS_2^A and TS_2^B, relative to the morpholine and piperidine products respectively. For TS_2^A a study was then carried out on diastereoselectivity of the reaction by reversing the configuration of the ketonic carbon after the cyanide attack, thus obtaining $TS_{2(R^*, S^*)}^A$ and **$TS_{2(R^*, R^*)}^A$** (Figure 19, pathway A). For **TS_2^B** it would be necessary to carry out a study on all four possible diastereoisomers that can be generated by the forging three stereocenters in the final piperidine cycle. However, as the determining stage of the reaction is the first, it is sufficient to evaluate **TS_2^B** for only one of the possible piperidine diastereoisomers (Scheme 8 pathway B). For the second cyclization step, the activation energy values are shown in Table 2.

Table 2- Energies related to the second cyclization step that leads to the morpholine or piperidine cycle. Both possible diastereoisomers are reported for the morpholine product.

	Opt EE (B3LYP) (a.u.)	H_corr (B3LYP) (a.u.)	SP EE (MO6-2X) (a.u)	SP+H_corr (a.u)	Rel H (Kcal/mol)
Int_1^A	-1488.146006	0.449945	-1488.009194	-1487.559246	3.2
Int_1^B	-1488.160677	0.450335	-1488.024988	-1487.574653	-6.5
$TS_{2(R^*,S^*)}^A$	-1488.123089	0.448962	-1487.991059	-1487.542097	14.0
$TS_{2(R^*,R^*)}^A$	-1488.119706	0.449122	-1487.986434	-1487.537312	17.0
TS_2^B	-1488.140398	0.449923	-1488.012121	-1487.562198	1.4
Int_2^B	-1488.169785	0.451847	-1488.039844	-1487.587997	-14.8
$Int_{2(R^*,R^*)}^A$	-1488.130511	0.450793	-1488.001473	-1487.55068	8.6

Int$_{2(R^*,S^*)}^{A}$	-1488.137347	0.450735	-1488.007873	-1487.557138	4.5

It is noteworthy that the cyclization step is favorited for the piperidine adduct with respect to the morpholine one. However, by considering that the cyanide addition is the determining step and the **TS$_{2(R^*,S^*)}^{A}$** is 2 Kcal/mol more favorite than TS$_1^B$, pathway A is in any case preferred. In addition, **TS$_{2(R^*,R^*)}^{A}$** is 3 Kcal/mol higher in energy than **TS$_{2(R^*,S^*)}^{A}$**. This energy barrier neglected its formation in the reaction environment. In Table 2 the relative energies Rel E (Kcal/mol) are evaluated respect the activated complex A (**AC^A**). Scheme 8 shows the structures and their names used in Table 2. Below the two-dimensional representation are the structures of the three transition states (Figure 12) obtained through the *Gaussian*[28] calculation program.

Pathway A

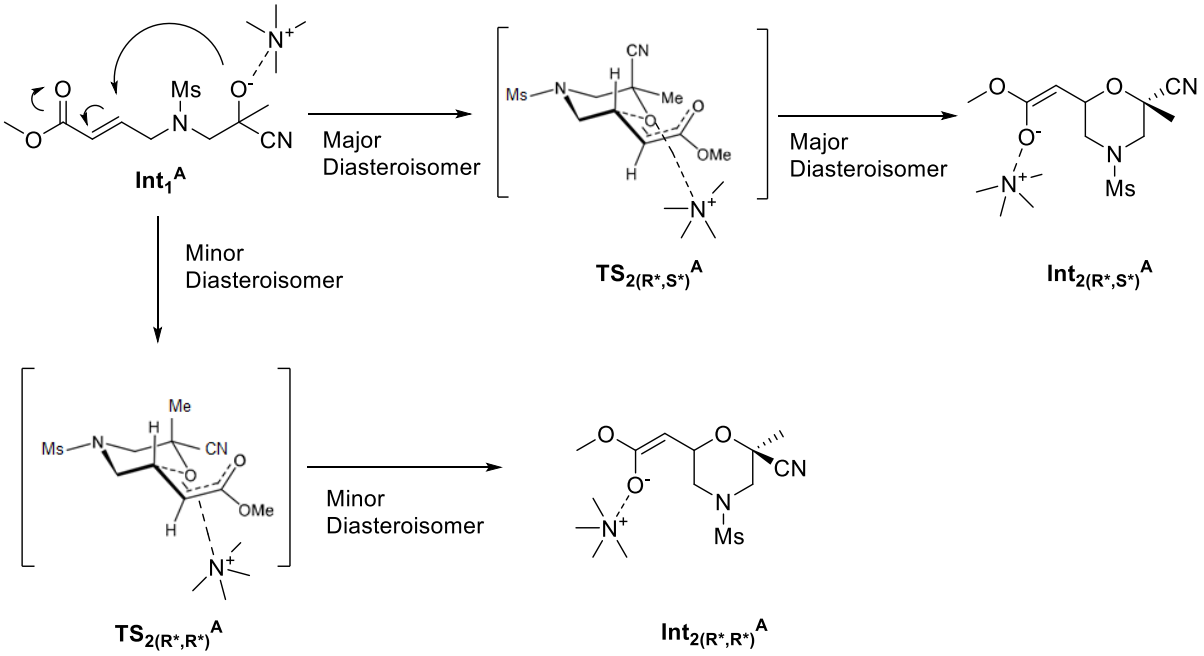

Pathway B

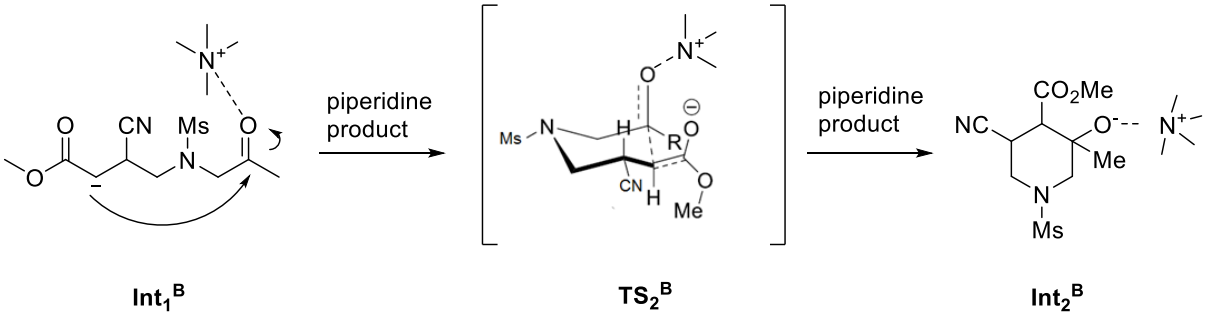

Scheme 8- Molecular species considered in Table 2.

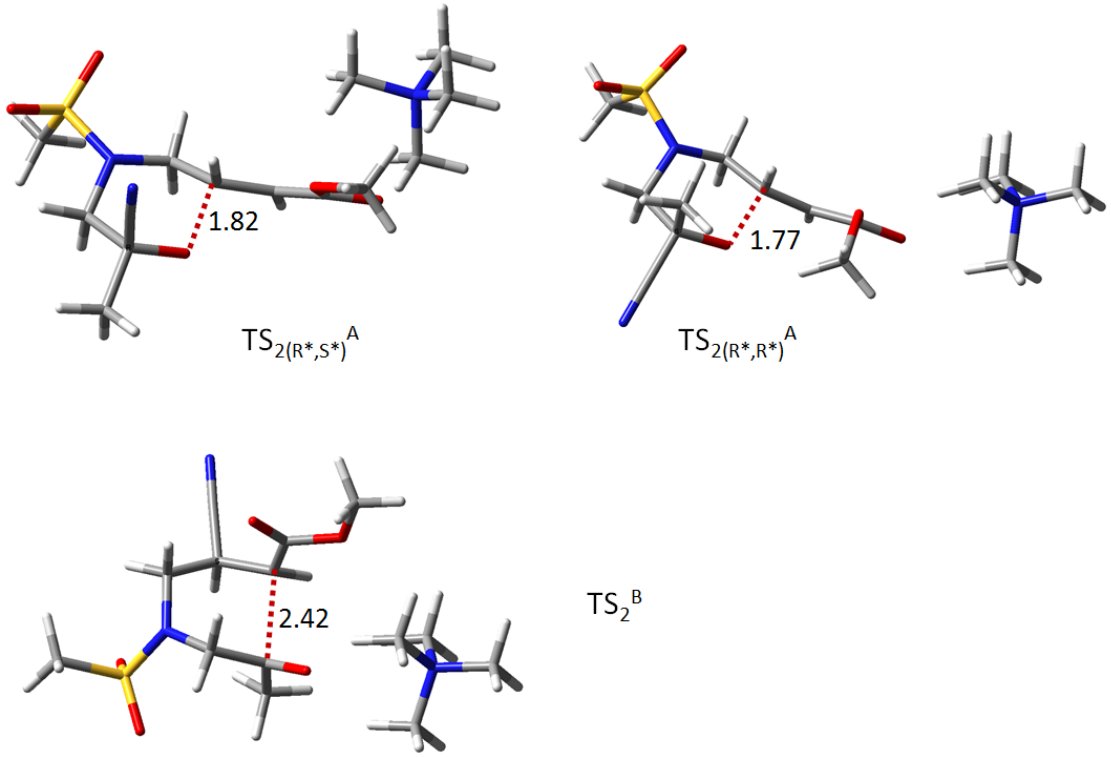

Figure 12- Three-dimensional representation of transition states leading to the formation of the two cycles.

The reaction turns to be endothermic with a $\Delta H = 4{,}5\ KCal$ and $\Delta H = 8{,}6\ KCal$ for $\mathbf{Int}_{(R^*,\ S^*)}^{A}$ and $\mathbf{Int}_{(R^*,\ R^*)}^{A}$ respectively. That is because, in this stage of the reaction, the product is an ester in its enolic form, which is unstable.

To complete the reaction it is also necessary to consider the final protonation step. The protonation TS has been obtained through an approach scan between the product in the enolic form and a water molecule. The successive IRC returns the energy of the protonates products, which is the ketonic form with a hydroxyl near the alpha carbon. To compare the energies of the various states, it is now sufficient to add an isolated water molecule to all stages of the reaction except the last one, or to subtract a water molecule only to the last step (see Scheme 9). This approach can be justified by the fact that water in the reaction has a single role in the final protonation of the enolic species while it can be considered isolated and non-reactive in previous stages. Considering also that errors in the calculations are proportional to the number of electrons in the system, the inaccuracy made in considering water isolated is lower than for the other possible reaction schemes.

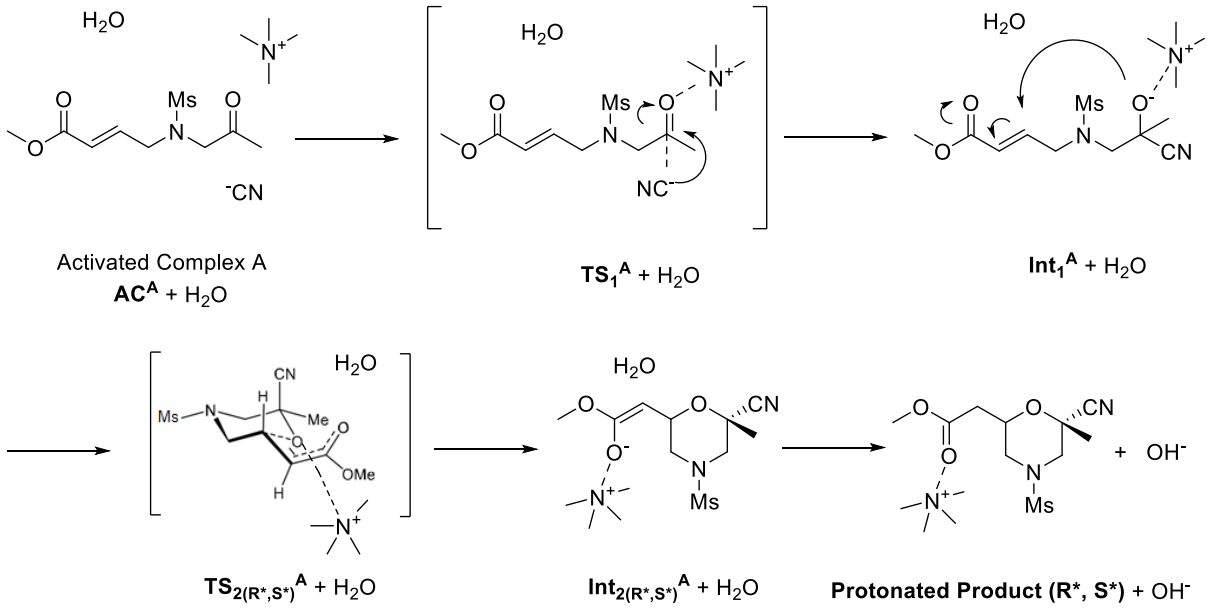

Scheme 9- Full reaction mechanism leading to the formation of the experimentally major product.

The same approach was also used for the minor diastereoisomers. Now is possible to graph the energy for this last step of the reaction for both pathway A and B. It is possible to notice that the protonated major diastereoisomer with relative configuration (R*, S*) is at an energy of -3.0 Kcal/mol from the activated starting complex. So the exothermicity of the reaction is confirmed.

Table 3- Energy values for the entire Pathway A and B.

	Opt EE (B3LYP) (a.u.)	H_corr (B3LYP) (a.u.)	SP EE (MO6-2X) (a.u)	SP+H_ corr (a.u)	Rel E (Kcal/ mol)
H_2O	-76.408954	0.024946	-76.411010	-76.386064	/
AC^A	-1488.151749	0.450066	-1488.014437	-1487.564371	0.0
AC^B	-1488.150941	0.449793	-1488.013469	-1487.563676	0.4
TS_1^A	-1488.131421	0.449261	-1487.996377	-1487.547116	10.8
TS_1^B	-1488.121723	0.448724	-1487.987185	-1487.538461	16.2
Int_1^A	-1488.146006	0.449945	-1488.009194	-1487.559246	3.2
Int_1^B	-1488.160677	0.450335	-1488.024988	-1487.574653	-6.5

$TS_{2(R^*,S^*)}^{A}$	-1488.123089	0.448962	-1487.991059	-1487.542097	14.0
$TS_{2(R^*,R^*)}^{A}$	-1488.119706	0.449122	-1487.986434	-1487.537312	17.0
TS_2^{B}	-1488.140398	0.449923	-1488.012121	-1487.562198	1.4
Int_2^{B}	-1488.169785	0.451847	-1488.039844	-1487.587997	-14.8
$Int_{2(R^*,R^*)}^{A}$	-1488.130511	0.450793	-1488.001473	-1487.55068	8.6
$Int_{2(R^*,S^*)}^{A}$	-1488.137347	0.450735	-1488.007873	-1487.557138	4.5
P.P.$_{(R^*,S^*)}$-H_2O	-1488.161334	0.453595	-1488.022658	-1487.569063	-3.0
P.P.$_{(R^*,R^*)}$-H_2O	-1488.160501	0.453633	-1488.021104	-1487.567471	-2.0

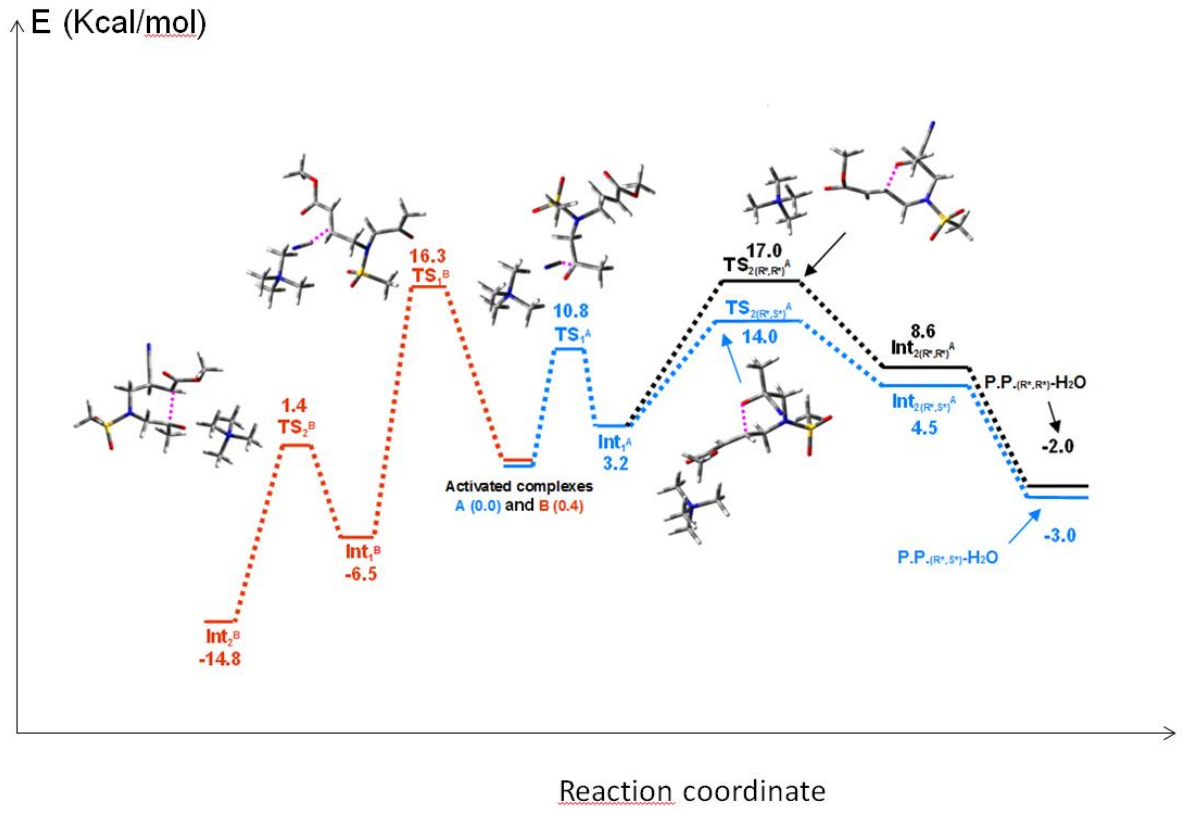

Figure 13- Energy-coordinate reaction chart with all possible steps that can occur for the reaction between cyanide and substrate.

4.2-Reaction with phenyl sulfide

The reaction between phenyl-sulfide and the substrate **1a** is a cascade sulfa-Michael/aldolic reaction. The experimental conditions used for this reaction are:

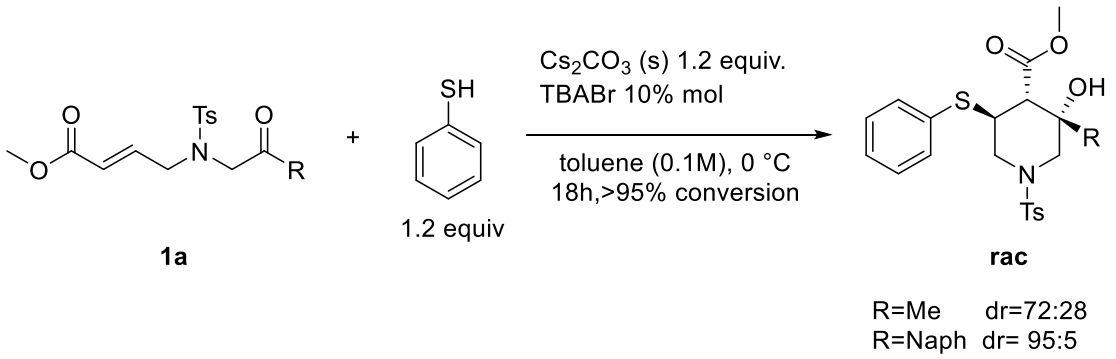

Scheme 10- Experimental conditions of the reaction of phenyl sulfide with substrate **1a**.

The reaction was conducted in the same experimental conditions of the one between cyanide and substrate **1a** using phenyl-sulfide as nucleophile, but it follows a different pathway. This reaction is also high diasteroselective and the conversion after 18h is over 95%, at 0°C. To simulate this mechanism, it was decided to modify substrate **1a** employing the same model used for morpholine formation. During the reaction that leads to the piperidine cycle, 3 chiral centers are formed, in positions 3,4,5 (see Scheme 11). The main diastereoisomer formed in the reaction has the relative configuration 3R*,4R*,5R*, while the minor diastereoisomer formed in the reaction, has the relative configuration 3R*,4S*,5S*. Relative configurations have been experimentally assigned by H-NMR spectroscopy, with NOE experiments.

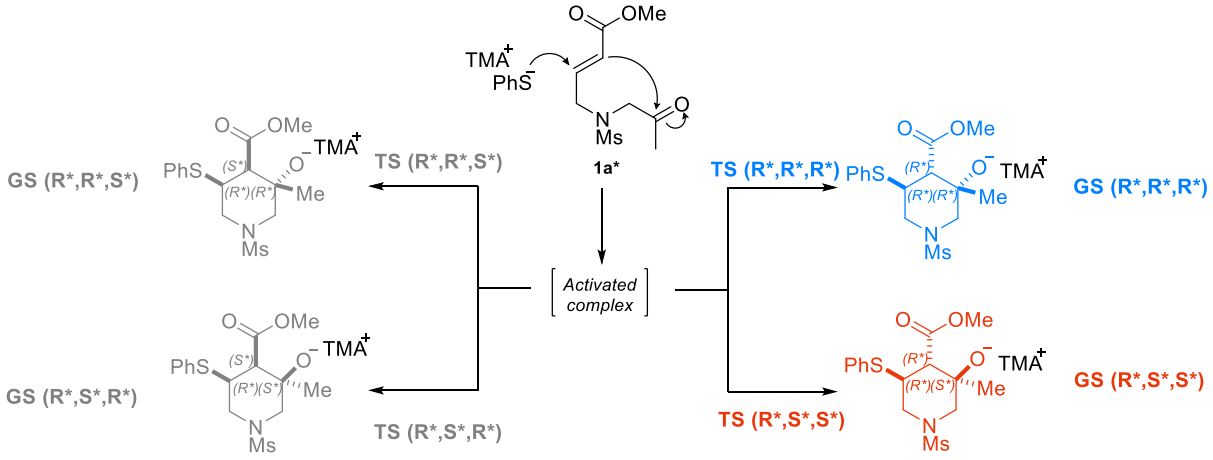

Scheme 11- Reaction scheme for the 1,4 addition of sulfide to the α,β-unsaturated ester site, and the 4 available diastereoisomers that can be formed.

4.2.1- Computational details

For this second nucleophile, both possible attacks on the electrophile sites of the substrate were evaluated. As for the cyanide, two scans have been performed. In the first, the sulfide is placed at a distance of about 4.2A from the ketone. In the second at the same distance from the double bond of the α,β-unsaturated. In the case of the nucleophile attack on the carbonyl, it was not possible to find any transition state for this reaction. The reason is that a soft nucleophile such as sulfur usually has too low charge density to attack the carbonyl of the ketone. The approach scan of sulfide and ketone only leads to an exponential increase in the energy of the system, without observing points where the gradient of system energy is zero. On the other hand, also the approach scan of the sulfide to the α,β-site in a staggered conformation doesn't achieve any valid transition state with an imaginary frequency.

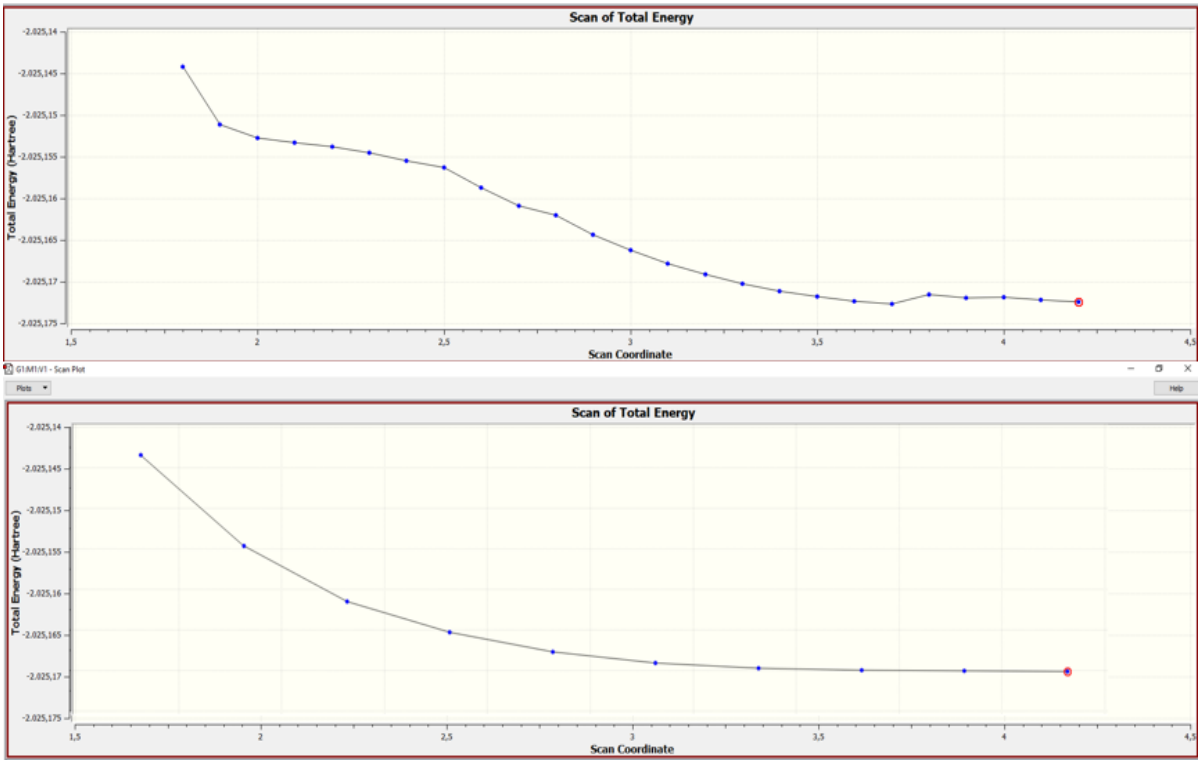

Figure 14- The first graph is the result of the approach scan of phenyl-sulfide and the β-carbon of the ester. The second graph is the result of the approach scan of phenyl-sulfide and ketone carbonyl.

This is in contrast with the experimental results. For this reason, a concerted transition state has been hypothesized. To find the concerted TS we start from the final product and ward off the two carbons involved in the last cyclization step. The result of the scan is a progressive extension of the bond between sulfur and the carbon in β position while the carbons are warding off (see in Figure 15):

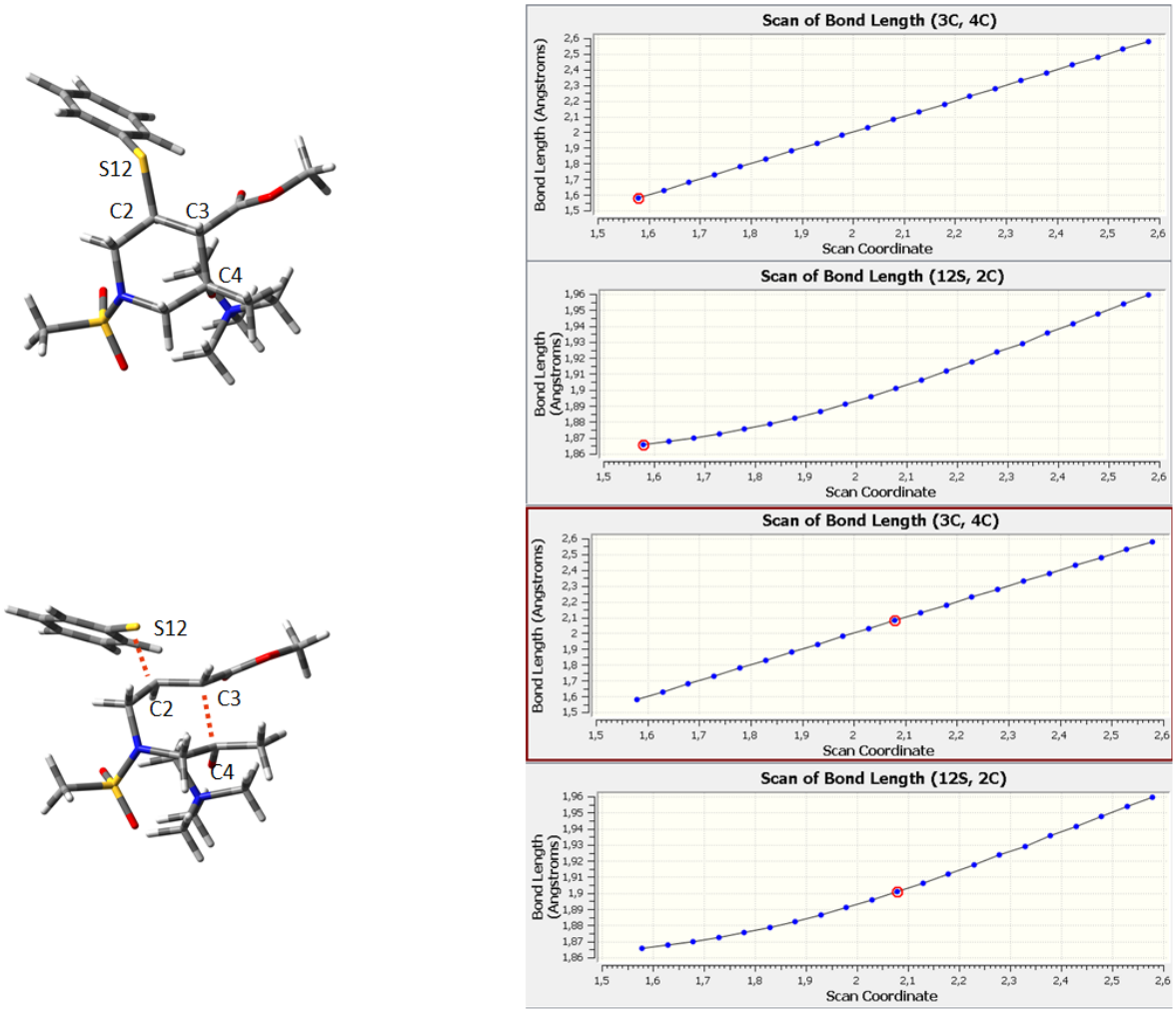

Figure 15- Trend of the bond distance between C and S when the C3-C4 bond is stretched.

Further lengthening of the bond between C3 and C4 led to the definitive detachment of sulfide from the β carbon. For this reason, the hypothesis of a concerted mechanism has been confirmed. The same scan for an evaluation of a concerted reaction that leads to the morpholine scaffold was performed. Pleasingly, the result has shown a disaggregation of various functional groups of the molecule, leading to the conclusion that the sulfide can't evolve to the morpholine product in these conditions.

The attack of sulfide to the β position of the ester leads to an alpha carbon activation that allows intramolecular aldolic reaction with ketone on the opposite side of the chain. Optimizing the transition state point with a zero-energy gradient obtained by the opening scan of the piperidine, we have found a TS with the concerted formation of both the bond between C3 and C4 and between S and C_β. The successive IRC calculation led to the piperidine product coordinated by the TMA and to the activated complex.

Since the reaction is diastereoselective, it is necessary to validate the experimental results obtained through the analysis of all 4 possible diastereomeric transition states. The evidence obtained in the experimental work is that only 2 of the 4 possible diastereoisomers are found in the mixture reaction. In particular, diastereoisomer with relative configuration 3R*,4R*,5R* was found to be the major diastereomer while 3R*,4S*,5S* the minor. For this reason, it was necessary to perform the scan for the C3-C4 binding, the optimization of the transition state and the subsequent IRC calculation for all the possible 4 diastereoisomers. The most stable activated complex is the one related to the formation of the most stable diastereoisomer $\mathbf{AC_{R*,R*,R*}}$ and was therefore taken as the reference energy to assess the activation energy of reactions. For each diastereoisomer, the catalyst is placed near the carbonyl of ketone. The energy trend of the 4 diastereoisomers is well represented by DFT simulations (results are reported in Table 5).

Table 5- Energies of transition states and ground states for the 4 piperidine diastereoisomers that can form.

	Opt EE (B3LYP) (a.u.)	H_corr (a.u.)	SP EE (M06-2X) (a.u.)	SP+H_corr (a.u.)	Rel. E. (kcal/mol)
$AC_{R*,R*,R*}$	-2025.174365	0.538571	-2024.994546	-2024.455975	0.0
TS R*,R*,R*	-2025.154888	0.537665	-2024.981022	-2024.443357	7.9
TS R*,S*,S*	-2025.151895	0.537752	-2024.980034	-2024.442282	8.6
TS R*,R*,S*	-2025.146750	0.537872	-2024.976547	-2024.438675	10.8
TS R*,S*,R*	-2025.148712	0.538166	-2024.978309	-2024.440143	9.9
GS R*,R*,R*	-2025.174669	0.539680	-2025.003465	-2024.463785	-4.9
GS R*,S*,S*	-2025.151895	0.537752	-2024.995082	-2024.457330	-0.9
GS R*,R*,S*	-2025.164061	0.539817	-2024.995752	-2024.455935	0.0
GS R*,S*,R*	-2025.148712	0.538166	-2025.002416	-2024.464250	-5.2

It is possible to note that diastereoisomer R*,R*,R* has the lowest energy transition state, while the experimental minor diastereoisomer has a transition state 0.7 Kcal/mol higher in

energy. The other two diastereoisomers are related to TS that is higher in energy (>2,0 Kcal/mol) and so they are not formed at 0°C. This is fully consistent with the experimental results. The lower energy for the **$TS_{(R^*,R^*,R^*)}$** can be explained through the geometry of the transition state. In this diastereoisomer, the location of the catalyst plays a key role in determining the energy of the system. The tetramethylammonium during the removal scan of the two carbon passes from a position close to the oxygen of the ketone to a position between the two carbonylic oxygens. This catalyst location activates both carbonyls and this is possible only in the transition state related to the formation of the R*,R*,R* diastereoisomer (see Scheme 12 and Figure 16). In addition to the stabilization the oxygen of the ketonic carbonyl, the TMA also interacts with the oxygen of the ester. The transition state leading to the minor diastereoisomer R*,S*,S* is characterized by the interaction between TMA and the oxygen of the ketonic carbonyl and a partial interaction between the catalyst and oxygen of the methoxy group. For this reason, it is possible to explain the diastereomeric excess. Finally, it was not necessary to assess the final protonation state. The anion obtained in this case is an alkoxide, a stable molecule (or sufficiently stabilized by tetramethylammonium), so the reaction is characterized by an exothermic profile.

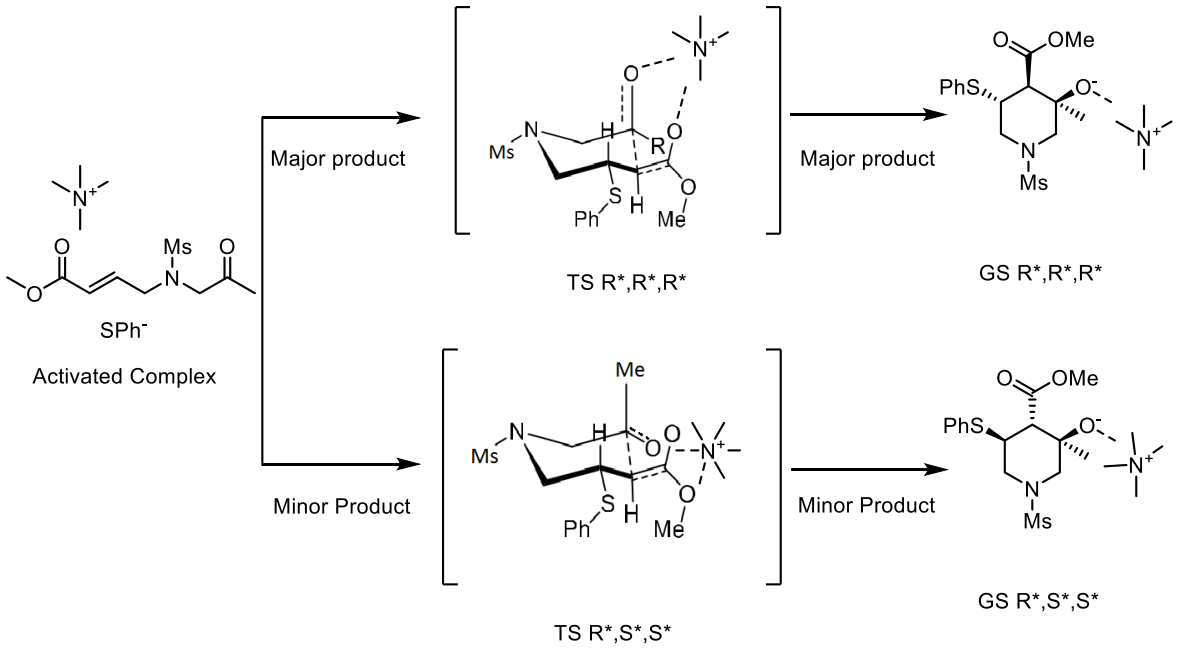

Scheme 12- Two-dimensional representation of the chair transition states leading to the major and minor diastereoisomer.

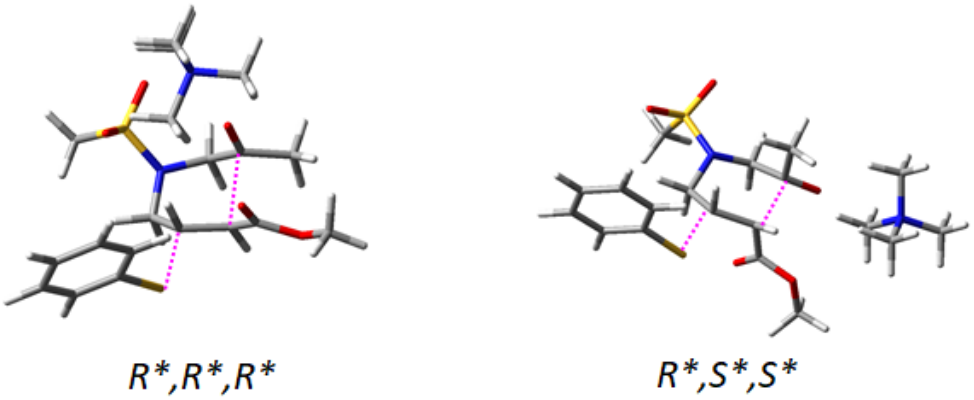

Figure 16- Three-dimensional representation of the chair transition states leading to the major and minor diastereoisomer.

Among the final piperidine product, the R*,S*,R* diastereoisomer is the most stable with an energy of 5.2 Kcal/mol lower than the $\mathbf{AC_{R*,R*,R*}}$ and 0.3 Kcal/mol lower than the R*,R*,R* piperidine diastereoisomer. However, $\mathbf{TS_{R*,S*,R*}}$ derives from a transition state that is 2.0 Kcal/mol higher than the major diastereoisomer and for this reason, at low-temperature, it can't be formed. Figure 17 reported the energy graph for all the 4 possible diastereoisomers that can be formed. Furthermore, by analyzing the structure of the transition states it is possible to understand why an increasing the steric hindrance on the ketone increases the diasteroselection of the reaction. In the TS that leads to the formation of the R*,R*,R* diastereoisomer the catalyst is placed above the two parallel carbonyls. This situation is not particularly affected by the presence of a bulky substitute on the ketone as it is widely distant from the catalyst. Otherwise, in the transition state of diastereoisomer R*,S*,S* the tetramethyl ammonium catalyst is located in a position close to the ketone. The presence of a bulky group such as a naphthyl leads to a lower catalytic function of the TMA. This is experimentally highlighted by an increase in the diasteroselection from dr=72:28 in the case of methyl ketone to a dr=95:5 in the case of naphthyl ketone.

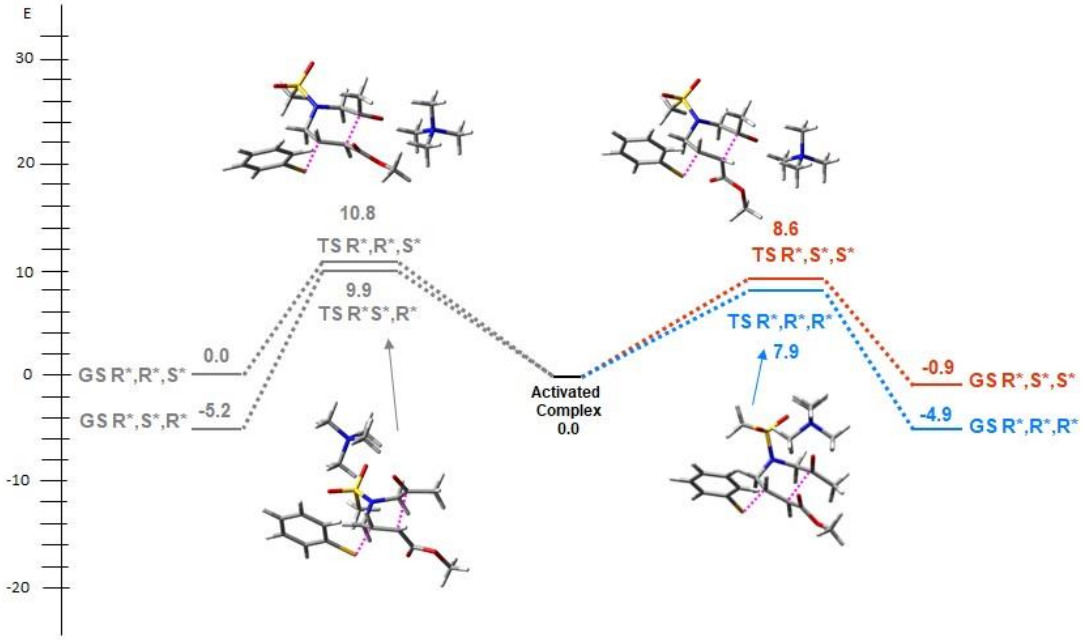

Figure 17- Full chart for the phenyl sulfide-substrate reaction.

4.3-Comparison of experimental and computational data

It is possible to compare the diastereoisomeric ratio obtained experimentally with the Boltzman's populations of their respective transition state. It is possible to apply:

$$P(product,i).=\left(\frac{e^{\frac{-Ea_{TSi}}{RT}}}{\sum_i^n e^{\frac{-Ea_{TSi}}{RT}}}\right) \tag{43}$$

In which Ea_{TSi} is the activation energy of the transition state that leads to the i-th product. For the reaction between cyanide and substrate, the mixture of the end products is composed of a single morpholine diastereoisomer. For pathway A, which leads to the formation of the morpholine cycle, it was calculated that the determining stage of the reaction is the cyclizzation step. For this reason, two possible diastereoisomeric transition states ($\mathbf{TS_{2(R*,S*)}^{A}}$ and $\mathbf{TS_{2(R*,R*)}^{A}}$) have to be evaluated. For pathway B that leads instead to the formation of the piperidine cycle, the determining step of the reaction turns out to be the addition of cyanide to the αβ-unsaturated site of the ester. So is necessary to compare three transition states together and asses what is the statistically preferred product of the reaction. In table 6 there are the results applying the equation (43).

Table 6- Population of the various the TS for cyanide-substrate reaction

	Ea (KCal/mol)	P(product,i)
$\mathbf{TS_{2(R^*,S^*)}^{A}}$	14.0	0.97
$\mathbf{TS_{2(R^*,R^*)}^{A}}$	18.0	0.01
$\mathbf{TS_{1}^{B}}$	16.2	0.02

Comfortably, the main product obtained experimentally is the one related to the most populated TS (0,97).

For the reaction between phenyl sulfide, the transition states to be compared are four, those related to the possible diastereoisomers that can be formed. It is not necessary to compare other TS because only the concerted cyclization pathways leading to the formation of piperidines have been found.

Table 7- Population of the various TS for the phenyl sulfide-substrate reaction.

	Ea (KCal/mol)	P(product,i)
R*,R*,R*	7.9	0.73
R*,S*,S*	8.6	0.23
R*,R*,S*	10.8	0.01
R*,S*,R*	9.9	0.03

In Table-7 there are shown the population of the four transition states. The results are close to the experimental ones in witch the R*,R*,R* diastereoisomer is the major one with a dr=72:28. The Boltzman populations of the other two TS are 0,01 and 0,03, two small to be observed experimentally.

5-Conclusions

Thanks to the computational study carried out it was possible to evaluate the mechanism that leads to the formation of the piperidine and morpholine heterocycles varying the nucleophile from the same starting **1a**. For the nucleophilic addition of cyanide both the possible pathways have been analyzed. The one that leads to the formation of the morpholine cycle and the one that evolves towards the formation of piperidine. It has been shown that the determining stage for this reaction is the cycloaddition following to the nucleophilic addition. In particular, cycloaddition is at an energy of 2 Kcal/mol lower than the addition of the cyanide to the β-carbon of the ester, leading to the preference of morpholine product respect to the piperidine one. The diasteroselection of the reaction resulting in the experimental data is not directly related to the position of the catalyst but for the steric hindrance during the transition state. As regards to the nucleophilic addition of phenyl sulfide, it hasn't been possible to find any transition states that lead to the formation of morpholine products. This probably depends on the "soft" character to the phenyl sulfide nucleophile that disfavours the addition of the ketonic site. Consequently, the reaction that leads to morpholine cannot occur. Concerning the evaluation of the mechanism leading to the formation of the piperidine cycle the transition state of the unconcerted addition was not found, for this reason, a concerted mechanism has been hypothesized. The subsequent scan of stretching the bond between atoms involved in the cyclization led to the simultaneous removal of the sulfide tied to beta carbon, confirming the hypothesis of the concerted mechanism. The diasteroselection of the reaction was explained by the energy evaluation of the transition state for all the possible diastereoisomers that can form in the reaction. The lower energy of the TS related to the formation of the diastereoisomer R*, R*, R* is caused by the parallel disposition of the two carbonyls in this diastereoisomer during the formation of the bond. This conformation allowing the catalyst to position itself in position between the two carbonyls and to activate both reaction sites. The increase in the diastereoisomeric ratio due to an increase of hindrance on the ketone can be explained in the same way. Finally, we have demonstrated that computational results are fully consistent with the experimental ones.

6-Experimental section

All the calculations were performed with the Gaussian 16 suite program using DFT and two different computational levels (B3LYP/6-31G(d) and M06-2x/6-311+G(d)). All the ground and transition states (GS and TS respectively) were validated by frequency analysis showing no immaginary frequencies for the GS and a single negative frequency for the TS. The normal mode corresponding to the negative frequency was visualized with Gaussianview[30] to check whether it corresponded to the correct reaction pathway. Each TS was validated showing that the displacement vectors related to the single negative frequency were related to the association or dissociation mechanism of the bonds involved in the reaction. The key stationary point for the reaction pathway were connected through an IRC calculation performed at B3LYP/6-31G(d) level. Single point energies were obtained with M06-2x/6-311+G(d) and the final energies to compared for the determination of the best reaction pathway were obtained by addng the ZPE contribution to the Enthalpies evaluated at the lower calculation level to the sngle point energy. In all the manuscript the reported energies are ZPE-corrected enthalpies in standard conditions (298K and 1 atm). The use of enthalpy provides less accurate absolute energy for the TS with respect to GS, but a more reliable comparison within them.

6.1-Reaction with phenyl sulfide

The reaction between phenyl-sulfide and the substrate **1a** is a cascade sulfa-Michael/aldolic reaction. As first attempt, the intramolecular TS was serched starting from the cyclized compound (with S, S, S absolute configuration) by a relaxed scan of the potential energy surface (PES) that accounted for the elongation of the C3-C4 bond. The geometry corresponding to the energy maximum was then used as imput for the optimization of the TS geometry. It was found that the reaction coordinate related to the immaginary frequency involved also the formation of the S-C_β bond. From this geometry, an IRC calculation confirmed that the TS connect the cyclized compound and the starting reagents. Several attempts were made to localize the TS for the alternative pathway where the PhS^- nucleophile adds to the ketone and the intermediate then cyclizes to yield a morpholine derivative. However, we cannot find any effective geometry for this TS. Once the TS for cyclization was found, we searched for the TS geometries leading to the three remaining diastereoisomers, in order to check whether the observed major diastereoisomer (*R**,*R**,*R** relative configuration) was indeed the one corresponding to the lowest energy TS.

6.2-Reaction with cyanide

In the case of the reaction with CN^- as nucleophile, a morpholine ring was obtained instead of piperidine. The reaction pathway A leads to the formation of the observed compound, while pathway B yields a piperidine derivative. The first reaction step for the formation of the morpholine ring involves the nucleophilic addition of CN^- to the ketone, followed by the nucleophilic addition of the oxygen on the β carbon of the α,β-unsaturated ester. The First TS for the formation of morpholine (**TS_1^A**) was successfully localized, and subsequent relaxed IRC calculation allowed to connect it with an activated complex and to intermediate **Int_1^A**. The pathway to **Int_1^B** by way of TS_1^B was modeled in the same way. When the two intermediates **Int_1^A** and **Int_1^B** are formed, subsequent cyclization leads to morpholine or piperidine. The intramolecular **$TS_{2(R*,S*)}^A$** and were serched starting from the cyclized morpholine compound by two relaxed scans of the potential energy surface (PES) that accounted for the elongation of the O-C6 bond. After cyclization, the enolate can be protonated by a water molecule to obtain the final compound. As for the phenyl-sulfide the intramolecular **TS_2^B** was serched starting from the cyclized piperidine compound by a relaxed scan of the PES that accounted for the elongation of the C3-C4 bond.

6.3-Cartesian coordinates of the analyzed molecular systems

All Calculation have been performed whit Charge=0 and Spin Multiplicity=1

Ciano-addition

Activated complexes A (AC^A)

C	2.02014	1.50898	-0.48139
C	2.8286	0.29824	-0.85337
C	3.96413	-0.06539	-0.24709
C	0.59114	1.12147	2.30819
C	0.34615	0.36914	0.99605
H	2.45734	-0.3026	-1.68182
H	2.44621	2.02172	0.38869
H	2.02232	2.20312	-1.32748

H	0.96634	-0.53506	0.96976
H	-0.68721	0.00117	1.01344
H	4.37585	0.4926	0.58988
C	4.72142	-1.25632	-0.70201
O	4.40873	-1.99295	-1.61655
C	0.54572	0.26958	3.54715
H	0.56759	0.90023	4.43867
H	-0.35638	-0.36422	3.51119
H	1.40788	-0.41122	3.56215
O	0.76971	2.33008	2.31705
O	5.8339	-1.42832	0.05112
C	6.64147	-2.56151	-0.30127
H	6.9926	-2.4773	-1.33341
H	7.48248	-2.54944	0.39267
H	6.07	-3.48791	-0.19719
S	-0.59016	2.0366	-0.9471
O	-1.83537	1.25766	-0.81713
O	-0.09897	2.41684	-2.27496
N	0.61627	1.13744	-0.21977
C	-0.83511	3.56165	-0.01234
H	-1.61988	4.11903	-0.5295
H	-1.12191	3.31791	1.00927
H	0.09909	4.12466	-0.01126
N	-4.41253	-1.44324	-0.7404

C	-5.12198	-2.61415	-0.10782
H	-4.61404	-2.81898	0.84345
H	-6.16798	-2.34035	0.04808
H	-5.05563	-3.46606	-0.78839
C	-4.49393	-0.26061	0.19939
H	-3.93248	0.56502	-0.2373
H	-5.54863	-0.00277	0.3207
H	-4.04563	-0.56838	1.14777
C	-2.96326	-1.8157	-0.9631
H	-2.93609	-2.64443	-1.67432
H	-2.44033	-0.94213	-1.35345
H	-2.55274	-2.10749	0.00687
C	-5.04285	-1.08655	-2.04919
H	-6.08733	-0.81656	-1.88048
H	-4.50215	-0.2414	-2.47895
H	-4.98505	-1.9467	-2.71927
C	-2.1263	-1.59981	2.49916
N	-3.042	-2.29258	2.22495

Activated complexes B (AC^{B})

C	1.20531	0.49801	0.75812
C	-0.55601	2.31752	0.57935
C	4.45385	0.8822	0.51767
C	3.32587	0.98039	-0.5193
H	1.70095	1.11542	1.51471

H	0.83104	-0.39865	1.28584
H	2.97825	2.02136	-0.58722
H	3.74663	0.73168	-1.49956
H	-0.14947	2.908	1.39591
C	-1.7973	2.80622	-0.0509
O	-2.51924	2.17211	-0.81009
C	5.563	1.91004	0.38757
H	5.95279	1.93711	-0.6374
H	5.17694	2.9133	0.61001
H	6.36971	1.67269	1.08358
O	4.45767	0.02467	1.37816
O	-2.07377	4.07345	0.32835
C	-3.27074	4.64227	-0.22164
H	-4.14675	4.05804	0.07438
H	-3.32961	5.65142	0.18686
H	-3.21707	4.67219	-1.31321
S	2.1093	-1.4042	-0.96824
O	3.18191	-1.43975	-1.97204
O	0.71361	-1.61826	-1.38351
N	2.19504	0.11724	-0.26
C	2.4784	-2.57999	0.34106
H	2.5391	-3.56175	-0.13598
H	3.43199	-2.29545	0.78756
H	1.65898	-2.55276	1.07179

C	0.01994	1.18647	0.15049
H	-0.41334	0.66954	-0.7011
C	-0.40307	-2.1598	2.1236
N	-1.5012	-2.56299	2.27449
N	-3.68219	-1.59634	-0.15581
C	-4.72607	-1.18248	-1.14441
H	-4.46938	-0.19332	-1.52835
H	-4.7507	-1.90783	-1.9602
H	-5.69686	-1.1512	-0.64536
C	-3.99868	-2.95349	0.41957
H	-4.00194	-3.68066	-0.39537
H	-3.22214	-3.17824	1.16206
H	-4.98612	-2.90756	0.88486
C	-3.62342	-0.58948	0.96978
H	-2.86262	-0.93682	1.67583
H	-3.36666	0.38015	0.54048
H	-4.6082	-0.55402	1.44194
C	-2.3345	-1.65127	-0.83951
H	-2.38529	-2.38722	-1.64399
H	-2.12369	-0.66182	-1.24405
H	-1.58765	-1.93922	-0.09849

TS_1^B

C	1.22821	0.07012	1.55168
C	0.20314	2.25599	0.77644

C	4.1643	0.32383	-0.40937
C	2.63789	0.35138	-0.54712
H	1.91109	0.72092	2.10777
H	0.92142	-0.73648	2.21669
H	2.22205	1.35388	-0.38901
H	2.37111	0.03866	-1.55997
H	0.82997	2.86494	1.42094
C	-0.65359	2.90577	-0.15238
O	-1.54165	2.3919	-0.85202
C	4.77068	1.1117	0.73154
H	4.52733	2.17652	0.62667
H	4.34513	0.78138	1.68697
H	5.85427	0.97896	0.74558
O	4.84607	-0.32616	-1.18363
O	-0.38904	4.25899	-0.25312
C	-1.19613	4.96343	-1.18811
H	-2.25995	4.88966	-0.93652
H	-0.87252	6.00611	-1.13533
H	-1.05984	4.5819	-2.20642
S	1.38925	-1.99579	-0.16545
O	0.64467	-1.7728	-1.42263
O	0.69293	-2.67704	0.93587
N	2.02738	-0.55183	0.46163
C	2.8804	-2.91459	-0.5786

H	2.55183	-3.82718	-1.08104
H	3.51196	-2.31322	-1.23592
H	3.40395	-3.14844	0.34941
C	0.03163	0.86966	1.03713
H	-0.45505	0.35691	0.20619
C	-1.33417	0.44356	2.22254
N	-2.44786	0.29933	2.55961
N	-3.66853	-1.36078	-0.41677
C	-4.27055	-2.07267	-1.58797
H	-3.51441	-2.16238	-2.36976
H	-4.60091	-3.06456	-1.27335
H	-5.1203	-1.49535	-1.95692
C	-4.68622	-1.21192	0.68402
H	-5.02019	-2.20689	0.98628
H	-4.20787	-0.69097	1.51906
H	-5.52935	-0.63406	0.29982
C	-3.2017	0.01463	-0.84498
H	-2.83754	0.56	0.02168
H	-2.39667	-0.09164	-1.57058
H	-4.04715	0.54261	-1.28946
C	-2.4901	-2.15299	0.10017
H	-2.83486	-3.15779	0.35299
H	-1.7212	-2.19324	-0.67214
H	-2.10374	-1.65133	0.98653

TS_1^A

C	2.03853	1.09981	1.05189
C	3.11824	0.54406	0.16032
C	3.92503	-0.46486	0.51056
C	-0.85193	-0.89557	1.24505
C	0.10269	-0.27374	0.19418
H	3.23485	1.00985	-0.81574
H	2.00523	0.55364	2.00012
H	2.27025	2.14358	1.28754
H	0.92466	-0.9928	0.07102
H	-0.42957	-0.24096	-0.75459
H	3.84306	-0.95923	1.47553
C	4.9839	-0.95498	-0.4022
O	5.22113	-0.53528	-1.51727
C	-0.34817	-0.91762	2.68977
H	-1.14465	-1.27838	3.34566
H	0.48855	-1.62804	2.75319
H	-0.01807	0.06557	3.03598
O	-1.47381	-1.91039	0.81908
O	5.68071	-1.96561	0.17777
C	6.73469	-2.51558	-0.62423
H	7.47342	-1.74753	-0.87005
H	7.18633	-3.30162	-0.01777
H	6.33572	-2.92957	-1.55457

S	0.26453	2.34118	-0.55229
O	-0.70404	1.8496	-1.54161
O	1.50031	3.00687	-0.99251
N	0.68536	1.04982	0.46403
C	-0.58903	3.49364	0.53764
H	-0.8352	4.37046	-0.06637
H	-1.48625	3.0077	0.92237
H	0.08827	3.77477	1.3467
N	-4.65465	-1.31944	-0.75626
C	-5.11299	-2.50413	-1.54914
H	-6.05564	-2.86939	-1.13692
H	-5.25067	-2.20765	-2.59072
H	-4.35002	-3.28115	-1.48074
C	-4.48427	-1.73076	0.69318
H	-3.60529	-2.37055	0.78074
H	-4.29897	-0.82755	1.27381
H	-5.405	-2.22831	1.00627
C	-3.34448	-0.81839	-1.33379
H	-3.12018	0.14762	-0.88475
H	-2.55397	-1.51684	-1.0494
H	-3.46783	-0.72889	-2.415
C	-5.67007	-0.21399	-0.82759
H	-6.62106	-0.57959	-0.43385
H	-5.29724	0.61493	-0.22225

H	-5.7872	0.09274	-1.86911
C	-2.16288	0.60397	1.43164
N	-3.20011	1.15187	1.35967

Int_1^A

C	1.9991	1.44614	0.84439
C	2.95828	0.73201	-0.06979
C	3.92158	-0.0963	0.35112
C	-1.03059	-0.24472	1.94224
C	0.09527	-0.21883	0.84189
H	2.84532	0.91812	-1.13618
H	2.1929	1.18431	1.89041
H	2.14062	2.52547	0.74075
H	0.96282	-0.82289	1.13179
H	-0.3017	-0.64608	-0.08147
H	4.07513	-0.31159	1.40573
C	4.83861	-0.75655	-0.60618
O	4.80913	-0.65193	-1.81656
C	-0.43337	0.103	3.32934
H	-1.22633	0.05204	4.08088
H	0.38853	-0.56044	3.6304
H	-0.06875	1.13523	3.29302
O	-2.09805	0.50578	1.62921
O	5.74586	-1.52054	0.05372
C	6.68647	-2.20758	-0.78279

H	7.27079	-1.49533	-1.37213
H	7.33295	-2.76403	-0.1031
H	6.17026	-2.88846	-1.46546
S	-0.21244	2.09492	-0.57426
O	-1.04348	1.23174	-1.43587
O	0.80111	2.96114	-1.19598
N	0.58437	1.1416	0.56647
C	-1.31213	3.11798	0.41194
H	-1.96126	3.66357	-0.27803
H	-1.85334	2.41649	1.06188
H	-0.69532	3.81456	0.98389
N	-4.12764	-1.1531	-1.1351
C	-4.69875	-2.14818	-0.16029
H	-4.05216	-2.19016	0.71825
H	-5.70659	-1.82848	0.11119
H	-4.73166	-3.12858	-0.64043
C	-4.08001	0.21553	-0.48721
H	-3.7241	0.92302	-1.23722
H	-5.09651	0.46384	-0.17213
H	-3.36353	0.20239	0.36429
C	-2.72923	-1.58004	-1.51043
H	-2.79757	-2.47437	-2.13364
H	-2.23866	-0.76076	-2.03631
H	-2.18949	-1.80444	-0.59223

C	-4.97969	-1.10085	-2.36577
H	-5.97687	-0.75242	-2.09078
H	-4.52671	-0.40614	-3.07486
H	-5.04049	-2.0982	-2.80674
C	-1.475	-1.71487	1.96482
N	-1.98659	-2.75642	1.84013

Int_1^B

C	1.64551	0.54483	1.32562
C	-0.01681	2.38957	0.55298
C	3.28907	0.52181	-1.4858
C	1.80505	0.34905	-1.17584
H	2.5177	1.19763	1.21114
H	1.84209	-0.11319	2.17682
H	1.29604	1.32565	-1.15621
H	1.34199	-0.23242	-1.97943
H	0.56927	3.29766	0.46092
C	-1.22646	2.30492	-0.10734
O	-2.10537	1.38332	-0.04497
C	3.60813	1.36978	-2.70117
H	2.98785	1.08643	-3.55973
H	3.38573	2.422	-2.48038
H	4.6657	1.27346	-2.95453
O	4.15937	0.0277	-0.79029
O	-1.45813	3.37757	-0.97083

C	-2.69678	3.37426	-1.65183
H	-3.54916	3.3689	-0.96095
H	-2.7153	4.29539	-2.24162
H	-2.79987	2.51352	-2.32703
S	1.43347	-1.92816	0.24165
O	1.10454	-2.44817	-1.0971
O	0.54447	-2.24331	1.37374
N	1.51073	-0.27509	0.10861
C	3.0673	-2.55217	0.6886
H	2.98255	-3.63903	0.75795
H	3.77921	-2.24589	-0.0763
H	3.34834	-2.13069	1.6554
C	0.36374	1.38668	1.60719
H	-0.45777	0.6692	1.70797
C	0.54154	2.02344	2.9326
N	0.70525	2.53859	3.96216
N	-3.212	-1.62141	-0.2396
C	-3.69354	-3.03462	-0.32666
H	-2.85543	-3.7028	-0.12192
H	-4.48288	-3.18932	0.41176
H	-4.08075	-3.21952	-1.33075
C	-4.34184	-0.65828	-0.49668
H	-5.10799	-0.80937	0.26686
H	-3.92206	0.35038	-0.44318

H	-4.75565	-0.8643	-1.48639
C	-2.13165	-1.38037	-1.26951
H	-1.8206	-0.33771	-1.14833
H	-1.30186	-2.06445	-1.08895
H	-2.56377	-1.55837	-2.2573
C	-2.65357	-1.35027	1.14021
H	-3.43295	-1.57821	1.87097
H	-1.77283	-1.97565	1.29437
H	-2.37803	-0.292	1.15579

TS_2^B

C	2.458	1.08659	-0.34974
C	1.6333	1.58753	0.86372
C	0.13437	1.34322	0.74088
C	-0.05446	-1.00017	0.17145
C	0.97305	-0.86436	-0.95547
H	2.00734	1.05217	1.74522
H	2.12974	1.6196	-1.24397
H	3.51641	1.29784	-0.1788
H	1.09418	-1.85634	-1.40603
H	0.5557	-0.19413	-1.7135
H	-0.40486	1.35933	1.68474
C	-0.55202	1.91596	-0.36601
O	-0.09766	2.22614	-1.47237
C	0.39778	-1.5128	1.52742

H	0.55963	-2.59715	1.44447
H	1.33042	-1.07323	1.88172
H	-0.38849	-1.33891	2.26768
O	-1.93088	2.05749	-0.14009
C	-2.60685	2.75045	-1.18448
H	-2.17513	3.74241	-1.35019
H	-2.56439	2.20515	-2.13416
H	-3.64642	2.85766	-0.8551
S	3.49435	-1.39523	-0.08203
O	2.95763	-2.75916	-0.1756
O	4.08264	-0.90214	1.17113
N	2.29665	-0.35297	-0.59103
C	4.77166	-1.23267	-1.35086
H	5.60875	-1.86854	-1.05341
H	4.35771	-1.56258	-2.305
H	5.09477	-0.19138	-1.40698
O	-1.24046	-1.22975	-0.19164
N	-4.40695	-1.05353	0.15029
C	-3.94	-2.47431	0.35144
H	-4.38503	-3.09921	-0.42562
H	-2.84852	-2.46297	0.28102
H	-4.2716	-2.80966	1.33639
C	-3.96358	-0.58047	-1.21607
H	-4.31162	0.44354	-1.35262

H	-2.87144	-0.62947	-1.24401
H	-4.41615	-1.2365	-1.96296
C	-3.77142	-0.18323	1.21082
H	-4.11847	-0.53269	2.18565
H	-2.69142	-0.2847	1.09844
H	-4.06593	0.85195	1.04208
C	-5.89838	-0.9818	0.25385
H	-6.34101	-1.61256	-0.51956
H	-6.20516	-1.33296	1.24087
H	-6.21342	0.05386	0.11468
C	1.94681	3.01726	1.09259
N	2.16961	4.14297	1.2797

$TS_{2(R^*,R^*)}^{A}$

C	0.51952	-0.01537	-0.31269
C	1.6725	-0.90977	-0.71338
C	3.44613	0.76335	-0.28737
C	2.39661	1.83335	0.12621
H	1.41641	-1.9431	-0.46689
H	0.34341	-0.00084	0.75931
H	4.37694	0.89923	0.26572
H	3.64053	0.87091	-1.36581
H	1.82831	-0.83202	-1.80137
N	2.90343	-0.56322	0.01698

O	1.17688	1.60813	-0.53114
S	3.99577	-1.7962	0.34885
O	5.01839	-1.23794	1.23606
O	3.21053	-2.97179	0.73392
C	-0.66092	-0.13249	-1.11469
H	-0.57453	-0.45997	-2.14692
C	-1.92646	0.22051	-0.67962
O	-3.01824	0.11126	-1.29821
O	-2.01566	0.72028	0.65436
C	-1.8946	2.14437	0.7232
H	-1.96871	2.41819	1.78058
H	-0.92792	2.46469	0.32114
H	-2.70507	2.63782	0.16646
C	4.81171	-2.19192	-1.21969
H	5.52817	-2.9916	-1.01914
H	4.06254	-2.53035	-1.93876
H	5.33281	-1.30534	-1.5873
N	-5.83408	-0.65481	0.17424
C	-5.24505	-1.75506	-0.67921
H	-4.26905	-1.40084	-1.0332
H	-5.15826	-2.65442	-0.06613
H	-5.92365	-1.9359	-1.51562
C	-5.89525	0.6156	-0.64263
H	-6.29849	1.40937	-0.0103

H	-4.87029	0.82862	-0.96997
H	-6.55604	0.44306	-1.49483
C	-7.20566	-1.04268	0.63182
H	-7.13856	-1.95824	1.22266
H	-7.61978	-0.23718	1.24122
H	-7.83819	-1.21007	-0.24186
C	-4.9432	-0.42061	1.37087
H	-3.95878	-0.08462	1.0261
H	-5.40964	0.34387	1.99627
H	-4.86372	-1.35652	1.92782
C	2.26755	1.92119	1.66375
H	2.00454	0.94197	2.07099
H	3.20715	2.24281	2.12612
H	1.48381	2.63924	1.92023
C	2.89788	3.14301	-0.37639
N	3.28837	4.16375	-0.76966

$TS_{2(R*,S*)}^{A}$

C	-0.30228	0.56105	0.16334
C	-1.05885	-0.72853	0.38753
C	-3.28738	0.34854	0.716
C	-2.63181	1.75269	0.66519
H	-0.60949	-1.51512	-0.22337
H	-0.46274	0.99507	-0.82053
H	-4.28624	0.35915	0.27575

H	-3.35837	0.07807	1.78294
H	-0.97291	-1.01242	1.44973
N	-2.47042	-0.62153	-0.02172
O	-1.32431	1.71235	1.12489
S	-3.23037	-2.03978	-0.5067
O	-4.53652	-1.67461	-1.05594
O	-2.25703	-2.80688	-1.29057
C	-3.42564	2.71743	1.56961
H	-2.96208	3.7063	1.53248
H	-4.47365	2.80192	1.26009
H	-3.37723	2.35152	2.60004
C	-2.70721	2.27549	-0.74197
N	-2.73417	2.71595	-1.81667
C	1.03806	0.59801	0.64179
H	1.29867	0.03284	1.5338
C	2.003	1.51948	0.19673
O	3.20726	1.57429	0.57059
O	1.56367	2.38751	-0.7719
C	2.51048	3.32477	-1.26579
H	1.94313	4.00719	-1.90205
H	2.99042	3.8761	-0.45195
H	3.29293	2.83801	-1.86362
C	-3.5467	-2.99064	1.00585
H	-4.04093	-3.91729	0.70589

H	-2.59753	-3.21332	1.49834
H	-4.20064	-2.41497	1.6643
N	4.77637	-1.32684	0.0753
C	4.68824	-0.89102	1.52049
H	4.05341	0.00494	1.54597
H	4.26456	-1.71275	2.10133
H	5.69803	-0.66604	1.87048
C	5.28018	-0.16536	-0.74943
H	5.29476	-0.46861	-1.79822
H	4.60246	0.67832	-0.57142
H	6.29152	0.07534	-0.41495
C	5.71034	-2.49039	-0.05929
H	5.34303	-3.31478	0.55467
H	5.7497	-2.79618	-1.10657
H	6.70401	-2.19038	0.2781
C	3.40114	-1.72713	-0.40456
H	2.69114	-0.90937	-0.23021
H	3.46329	-1.96656	-1.46796
H	3.09021	-2.61112	0.15614

$Int_{2(R^*,R^*)}$A

C	0.56182	0.30788	-0.27819
C	1.53844	-0.81778	-0.63219
C	3.46103	0.66877	-0.26737
C	2.47464	1.8031	0.11914

H	1.12408	-1.77183	-0.30496
H	0.33906	0.26761	0.79137
H	4.39253	0.75994	0.29346
H	3.67327	0.74895	-1.34533
H	1.68321	-0.84117	-1.72551
N	2.82494	-0.60733	0.05903
O	1.22677	1.60988	-0.54098
S	3.82108	-1.93582	0.31926
O	4.95008	-1.47026	1.12834
O	2.9593	-3.0322	0.76615
C	-0.68181	0.21943	-1.06775
H	-0.61551	-0.07725	-2.11121
C	-1.9169	0.57818	-0.59775
O	-3.03826	0.55321	-1.19269
O	-1.96159	0.98515	0.78064
C	-2.08642	2.39471	0.9215
H	-2.17008	2.60982	1.99213
H	-1.20249	2.90336	0.5155
H	-2.97989	2.77426	0.40528
C	4.48289	-2.40626	-1.30051
H	5.12566	-3.27557	-1.14529
H	3.65599	-2.66468	-1.96541
H	5.06637	-1.57714	-1.7066
N	-5.64565	-0.81267	0.10447

C	-4.94396	-1.66036	-0.93372
H	-4.04812	-1.10325	-1.24455
H	-4.69667	-2.62175	-0.47877
H	-5.63127	-1.80714	-1.76991
C	-5.91923	0.55111	-0.48722
H	-6.41263	1.16037	0.27324
H	-4.94531	0.96288	-0.78087
H	-6.57653	0.42413	-1.35013
C	-6.92664	-1.46592	0.51803
H	-6.70535	-2.44655	0.94388
H	-7.42258	-0.84107	1.26341
H	-7.56786	-1.57816	-0.35819
C	-4.74526	-0.646	1.30529
H	-3.83756	-0.1165	0.99793
H	-5.28848	-0.07159	2.05911
H	-4.50616	-1.63733	1.69575
C	2.33652	1.9431	1.64882
H	2.06635	0.98283	2.0928
H	3.28134	2.27283	2.09276
H	1.5615	2.67926	1.87825
C	3.01423	3.06998	-0.42963
N	3.4655	4.05599	-0.8433

$Int_{2(R^*,S^*)}$A

C	-0.38364	0.69646	0.19472

C	-1.04284	-0.68531	0.26077
C	-3.22997	0.35746	0.75423
C	-2.53489	1.73682	0.70047
H	-0.57665	-1.34604	-0.4699
H	-0.45864	1.08251	-0.82733
H	-4.25213	0.41766	0.37653
H	-3.2492	0.05524	1.81535
H	-0.89479	-1.1025	1.27256
N	-2.47928	-0.59436	-0.06502
O	-1.17153	1.61399	1.05478
S	-3.26805	-2.00807	-0.51693
O	-4.62592	-1.63804	-0.91968
O	-2.36693	-2.73234	-1.41632
C	-3.16655	2.69721	1.71767
H	-2.65545	3.66183	1.67283
H	-4.23182	2.84742	1.51539
H	-3.04055	2.28296	2.72242
C	-2.68637	2.32157	-0.6653
N	-2.81432	2.8182	-1.70676
C	1.02256	0.65022	0.63649
H	1.25059	0.11199	1.55424
C	2.00668	1.51517	0.16885
O	3.22237	1.55831	0.53309
O	1.59311	2.37301	-0.84018

C	2.57815	3.24029	-1.37592
H	2.03919	3.93684	-2.02319
H	3.10676	3.78816	-0.58988
H	3.32299	2.69852	-1.97655
C	-3.42161	-3.01061	0.98747
H	-3.92282	-3.93843	0.70325
H	-2.42635	-3.22714	1.38145
H	-4.02343	-2.47199	1.72262
N	4.68736	-1.37299	0.09766
C	4.63379	-0.89322	1.53048
H	4.02207	0.02118	1.53406
H	4.19807	-1.68677	2.1411
H	5.655	-0.68573	1.858
C	5.20445	-0.24715	-0.76752
H	5.19054	-0.57908	-1.80771
H	4.54829	0.61709	-0.59435
H	6.2283	-0.02518	-0.45856
C	5.58907	-2.56243	-0.01923
H	5.21233	-3.36002	0.62391
H	5.60275	-2.89843	-1.05797
H	6.59591	-2.27894	0.29278
C	3.2936	-1.75036	-0.34674
H	2.60151	-0.91206	-0.17988
H	3.33175	-2.01797	-1.40476

H	2.97484	-2.61402	0.24114

Int_2^B

C	-2.52639	0.8793	0.06104
C	-1.65178	1.68915	-0.9239
C	-0.13782	1.32817	-0.83297
C	0.1235	-0.23467	-0.91232
C	-0.85866	-0.95101	0.05996
H	-1.98339	1.43346	-1.93708
H	-2.28615	1.1809	1.08871
H	-3.58048	1.07529	-0.1403
H	-0.78145	-2.02607	-0.10775
H	-0.54596	-0.71888	1.08691
H	0.37974	1.79067	-1.67779
C	0.49436	1.8683	0.435
O	0.07761	1.71112	1.56699
C	-0.14331	-0.70746	-2.36045
H	0.06763	-1.78131	-2.42049
H	-1.17388	-0.55399	-2.70071
H	0.53924	-0.19078	-3.04569
O	1.60171	2.60266	0.16821
C	2.22264	3.19965	1.31355
H	1.52003	3.85403	1.83616
H	2.57052	2.4326	2.01268
H	3.06372	3.77681	0.92578

S	-3.47871	-1.62289	0.26137
O	-3.05471	-2.95199	-0.18563
O	-4.7502	-1.04214	-0.18044
N	-2.26316	-0.54638	-0.16608
C	-3.51359	-1.66114	2.07332
H	-4.29084	-2.36992	2.36737
H	-2.54086	-1.99267	2.44251
H	-3.75229	-0.66431	2.45026
O	1.40483	-0.50259	-0.52874
N	4.28886	-1.28665	0.0789
C	3.58434	-2.39969	-0.66339
H	3.61252	-3.29684	-0.04069
H	2.55574	-2.03532	-0.83041
H	4.11785	-2.57696	-1.59998
C	3.53471	-1.02112	1.36196
H	4.03432	-0.20493	1.88884
H	2.5086	-0.75431	1.06201
H	3.56357	-1.92921	1.96855
C	4.23997	-0.03823	-0.77399
H	4.7767	-0.24168	-1.7035
H	3.16993	0.16801	-0.94547
H	4.73288	0.76812	-0.22642
C	5.70377	-1.66491	0.37285
H	5.71262	-2.56679	0.9884

H	6.22579	-1.85337	-0.56745
H	6.18902	-0.84605	0.90807
C	-1.88025	3.12944	-0.74403
N	-2.04408	4.26997	-0.59674

P.P.$_{(R^*,R^*)}$

C	0.63454	0.54199	-0.18882
C	0.96762	-0.78976	-0.86259
C	3.29119	-0.04706	-1.12297
C	2.89796	1.32507	-0.49402
H	0.30497	-1.57077	-0.47612
H	0.77913	0.43999	0.89179
H	4.3191	-0.31037	-0.87102
H	3.20622	0.03877	-2.21263
H	0.78004	-0.70773	-1.94181
N	2.39402	-1.12711	-0.70678
O	1.50123	1.57593	-0.69898
S	2.83382	-2.10665	0.59601
O	4.29349	-2.01747	0.7198
O	1.97635	-1.85664	1.76477
C	-0.81015	0.89796	-0.47253
H	-1.38663	-0.02929	-0.18831
C	-1.43197	2.05481	0.25084
O	-2.53216	2.51079	-0.02548
O	-0.70257	2.50511	1.2926

C	-1.29023	3.57184	2.0504
H	-0.56257	3.81608	2.82501
H	-1.4776	4.43936	1.41226
H	-2.23478	3.2526	2.50045
C	2.40605	-3.74197	-0.03044
H	2.61352	-4.45287	0.7726
H	1.34436	-3.76276	-0.28411
H	3.0234	-3.95182	-0.90459
N	-4.93442	-0.8064	-0.34484
C	-4.06152	-0.35977	-1.49519
H	-3.96132	0.72657	-1.45487
H	-3.09137	-0.84094	-1.34819
H	-4.5392	-0.67616	-2.42571
C	-6.33483	-0.33337	-0.54893
H	-6.94609	-0.65337	0.29724
H	-6.33434	0.75665	-0.6147
H	-6.72838	-0.76229	-1.47332
C	-4.86785	-2.31392	-0.26566
H	-3.79418	-2.53697	-0.08921
H	-5.50698	-2.64184	0.55802
H	-5.23426	-2.72477	-1.20984
C	-4.36547	-0.24991	0.94273
H	-4.32618	0.83773	0.86353
H	-5.02012	-0.56152	1.76068

H	-3.35153	-0.70052	0.9976
C	3.29938	1.45269	0.98797
H	2.8646	0.64791	1.58496
H	4.3872	1.40482	1.09435
H	2.94205	2.41051	1.37545
C	3.59432	2.37896	-1.26722
N	4.17848	3.17803	-1.87267
H	-0.96876	1.05731	-1.54545
O	-2.02798	-1.74263	0.10448
H	-1.54906	-2.0756	0.88108

P.P.$_{(R^*,S^*)}$

C	-0.5876	0.87001	-0.61464
C	-1.21402	-0.51961	-0.77557
C	-2.59974	-0.08221	1.21043
C	-1.94051	1.30838	1.33236
H	-1.31429	-0.75458	-1.83758
H	-1.13271	1.6085	-1.21593
H	-3.63778	-0.04897	1.54515
H	-2.0258	-0.76123	1.86324
H	-0.54246	-1.25238	-0.29489
N	-2.5666	-0.50847	-0.18728

O	-0.63666	1.27923	0.76849
S	-3.59348	-1.77492	-0.62463
O	-4.85919	-1.55163	0.07726
O	-3.52769	-1.8869	-2.08186
C	-1.7634	1.70212	2.80351
H	-1.2797	2.67981	2.8678
H	-2.72981	1.74885	3.3141
H	-1.12645	0.96193	3.29629
C	-2.77534	2.33899	0.6512
N	-3.406	3.1768	0.15405
C	0.88702	0.78164	-0.98206
H	1.33175	0.00052	-0.33059
C	1.7103	2.0429	-0.90942
O	2.93055	2.05274	-0.86678
O	0.97566	3.16969	-0.94084
C	1.71005	4.40213	-0.89116
H	0.9575	5.19057	-0.91361
H	2.30046	4.45998	0.02726
H	2.38112	4.48527	-1.7505
C	-2.85058	-3.27903	0.06026
H	-3.47372	-4.11612	-0.26215
H	-1.83513	-3.39158	-0.32551
H	-2.84624	-3.21404	1.15037
N	4.61311	-1.50286	0.27427

C	4.23799	-2.84202	0.8661
H	3.1302	-2.80248	0.96128
H	4.57675	-3.6264	0.18437
H	4.7424	-2.94176	1.83068
C	4.08676	-0.42471	1.19749
H	4.26149	0.5476	0.73469
H	3.00318	-0.654	1.27049
H	4.6154	-0.51212	2.15026
C	6.08981	-1.37771	0.10469
H	6.445	-2.1725	-0.55537
H	6.31505	-0.40228	-0.33166
H	6.5697	-1.46583	1.08147
C	3.9216	-1.37283	-1.06312
H	2.86173	-1.57002	-0.87687
H	4.06661	-0.35474	-1.42862
H	4.36439	-2.10212	-1.74604
H	0.97314	0.40876	-2.01294
O	1.56547	-1.73609	0.61565
H	1.00108	-1.61277	1.39593

Solfur Addition

Activated Complex AC

C	3.06105	0.55037	-0.59828
C	2.14592	1.72075	-0.36665
C	1.59974	2.4629	-1.3371

C	1.91711	-2.24926	-1.60848
C	1.55594	-1.45307	-0.35369
H	1.95461	1.9697	0.67508
H	3.12613	0.29246	-1.66061
H	4.06404	0.83135	-0.25966
H	0.67193	-0.83303	-0.57703
H	1.23047	-2.14277	0.43144
H	1.78227	2.25628	-2.38783
C	0.73275	3.61951	-1.0345
O	0.26747	3.91185	0.05968
C	0.77392	-2.99948	-2.2469
H	0.35536	-3.73053	-1.54342
H	-0.04347	-2.30214	-2.47886
H	1.11879	-3.51075	-3.14805
O	3.05224	-2.24827	-2.0592
O	0.50429	4.34699	-2.1462
C	-0.32506	5.50638	-1.98692
H	0.07336	6.16246	-1.20877
H	-0.31601	6.00682	-2.95527
H	-1.34606	5.21448	-1.72369
S	3.6651	-1.23438	1.34782
O	2.87869	-2.18381	2.14169
O	4.31661	-0.07653	1.97159
N	2.62992	-0.61937	0.17938

C	4.95718	-2.17472	0.50385
H	5.61482	-2.57076	1.2813
H	4.49773	-2.97565	-0.07383
H	5.5086	-1.50514	-0.15807
C	-2.94112	-1.66378	-0.75534
C	-2.57206	-2.53954	0.29165
C	-3.3942	-3.59601	0.68816
C	-4.61943	-3.819	0.05689
C	-5.00472	-2.9653	-0.98185
C	-4.18558	-1.91052	-1.37915
H	-1.61794	-2.38514	0.79103
H	-3.07048	-4.2513	1.495
H	-5.25903	-4.64267	0.36334
H	-5.95397	-3.12456	-1.49022
H	-4.49444	-1.25837	-2.19162
S	-1.91188	-0.31163	-1.26705
N	-2.43806	1.88027	1.89634
C	-1.01677	1.37578	1.78574
H	-0.98862	0.6817	0.93557
H	-0.36685	2.23187	1.60119
H	-0.75862	0.87375	2.72065
C	-2.80696	2.60004	0.61983
H	-2.74224	1.86892	-0.19743
H	-3.8236	2.98482	0.7288

H	-2.09277	3.41076	0.46921
C	-3.36304	0.70538	2.08264
H	-3.08635	0.18797	3.00324
H	-4.38779	1.07608	2.15262
H	-3.25012	0.04284	1.2221
C	-2.55111	2.81776	3.05748
H	-2.279	2.28627	3.97155
H	-1.87104	3.65608	2.89776
H	-3.5799	3.17717	3.12747

GS (3R*,4S*,5S*)

C	-1.46586	0.61741	-0.53706
C	-1.16023	-0.62125	0.31345
C	0.34849	-0.93445	0.39982
C	1.20243	0.32823	0.85806
C	0.76584	1.55614	0.00694
H	-1.5156	-0.43471	1.33018
H	-1.19704	0.41903	-1.58295
H	-2.52783	0.85792	-0.47186
H	1.23168	2.44813	0.42823
H	1.13422	1.40131	-1.01597
H	0.50309	-1.71834	1.14637
S	-2.08907	-2.116	-0.29874
C	0.9256	-1.44389	-0.90773
O	0.86091	-0.89917	-1.9931

C	0.91481	0.60306	2.3522
H	1.53491	1.44721	2.67552
H	-0.12942	0.85587	2.56751
H	1.20035	-0.27249	2.94774
C	-3.77767	-1.71082	0.16114
C	-4.72512	-1.44284	-0.83571
C	-4.17618	-1.71263	1.50577
C	-6.05191	-1.17696	-0.49114
H	-4.41648	-1.44138	-1.87672
C	-5.49838	-1.42928	1.84656
H	-3.44943	-1.94172	2.27994
C	-6.43976	-1.16406	0.8491
H	-6.77924	-0.96941	-1.27166
H	-5.796	-1.42549	2.8919
H	-7.4708	-0.94889	1.11655
O	1.53992	-2.64576	-0.74428
C	2.07443	-3.21861	-1.94215
H	1.28879	-3.35932	-2.68954
H	2.84895	-2.57492	-2.37178
H	2.49582	-4.18146	-1.64755
S	-1.2842	3.28978	-0.30447
O	-0.45197	4.2384	0.44175
O	-2.73914	3.25746	-0.12408
N	-0.7004	1.75117	0.01483

C	-0.97863	3.59694	-2.06583
H	-1.34299	4.60235	-2.28794
H	0.09412	3.53234	-2.25936
H	-1.52331	2.85949	-2.65923
O	2.52967	0.08779	0.64662
N	5.53241	-0.31913	0.40342
C	5.22896	0.83834	1.32792
H	5.7038	1.734	0.92068
H	4.12719	0.91613	1.34635
H	5.64507	0.60788	2.31136
C	4.93289	-0.01376	-0.95066
H	5.13844	-0.85799	-1.61284
H	3.85281	0.12643	-0.77873
H	5.40985	0.88933	-1.33857
C	4.8638	-1.55884	0.95552
H	5.29363	-1.76615	1.93831
H	3.78728	-1.32061	1.01069
H	5.06925	-2.3882	0.27501
C	7.00686	-0.52645	0.28799
H	7.46555	0.38025	-0.11196
H	7.41582	-0.7428	1.27707
H	7.19859	-1.36592	-0.38364

GS (3R*,4S*,5R*)

C	0.78114	-0.25428	1.23052

C	1.19185	-0.32387	-0.24877
C	0.88568	-1.6792	-0.90793
C	-0.70192	-1.93768	-0.74614
C	-1.01714	-1.923	0.78685
H	0.61143	0.40821	-0.81324
H	1.40203	-0.94216	1.81655
H	0.91165	0.76344	1.60109
H	-2.093	-2.05454	0.90933
H	-0.48704	-2.72015	1.32591
H	1.05034	-1.5888	-1.98377
S	2.98556	0.12376	-0.44912
C	1.73851	-2.81303	-0.39506
O	1.9423	-3.10142	0.77255
C	-1.0454	-3.34315	-1.29339
H	-0.77511	-3.39549	-2.35344
H	-0.54416	-4.16544	-0.76546
H	-2.12866	-3.49617	-1.2161
C	2.91311	1.91645	-0.3556
C	3.4641	2.58207	0.74722
C	2.35978	2.66765	-1.40339
C	3.45756	3.97763	0.80337
H	3.89484	2.00178	1.55757
C	2.34193	4.06055	-1.33701
H	1.95614	2.15454	-2.27172

C	2.89278	4.71925	-0.23467
H	3.8878	4.48343	1.66383
H	1.91182	4.63399	-2.15459
H	2.88525	5.80502	-0.18831
O	2.24662	-3.54872	-1.41639
C	3.0224	-4.68882	-1.02421
H	3.87948	-4.38332	-0.41781
H	2.41486	-5.3911	-0.44571
H	3.35672	-5.15018	-1.95451
S	-1.5869	0.11394	2.49191
O	-2.99529	-0.17881	2.17638
O	-1.14872	1.51105	2.61906
N	-0.64609	-0.60942	1.34183
C	-1.23308	-0.70099	4.06976
H	-1.85643	-0.23354	4.8353
H	-1.47404	-1.76224	3.97908
H	-0.17571	-0.5643	4.30663
O	-1.37132	-0.96244	-1.39498
N	-3.55386	1.24191	-1.62362
C	-2.99155	0.88416	-2.97796
H	-2.23761	0.10238	-2.81165
H	-3.81143	0.52617	-3.6055
H	-2.55434	1.78445	-3.41638
C	-2.4188	1.71317	-0.74203

H	-1.96938	2.5934	-1.20821
H	-2.81731	1.96165	0.24174
H	-1.72277	0.86297	-0.68919
C	-4.14637	-0.00825	-1.01294
H	-5.00381	-0.30895	-1.62027
H	-3.33084	-0.74686	-1.03077
H	-4.44531	0.21215	0.0124
C	-4.59191	2.30719	-1.74831
H	-4.13617	3.20245	-2.17693
H	-5.3958	1.95214	-2.39692
H	-4.98709	2.53207	-0.75596

GS (R*,R*,S*)

C	-1.36418	1.35322	-0.73853
C	-1.22582	-0.11635	-0.3155
C	0.23974	-0.57554	-0.34369
C	1.21119	0.37195	0.50842
C	0.94696	1.81711	-0.01072
H	-1.63633	-0.25625	0.68571
H	-1.11664	1.43941	-1.81123
H	-2.39255	1.686	-0.59324
H	1.5274	2.51138	0.59832
H	1.30761	1.86867	-1.0529

H	0.62577	-0.51238	-1.36755
S	-2.26736	-1.1597	-1.4637
C	0.35969	-2.01009	0.11063
O	-0.22014	-2.50401	1.05993
C	0.8837	0.31356	2.01791
H	1.5816	0.97861	2.53949
H	-0.13408	0.63659	2.26144
H	1.02635	-0.70089	2.40012
C	-3.75071	-1.44323	-0.4926
C	-4.99301	-1.07089	-1.02133
C	-3.68938	-2.08912	0.75145
C	-6.16535	-1.34214	-0.31282
H	-5.03656	-0.56509	-1.98137
C	-4.86367	-2.33485	1.46274
H	-2.72644	-2.39389	1.15157
C	-6.10342	-1.96803	0.93262
H	-7.12542	-1.0492	-0.73007
H	-4.80958	-2.82722	2.4304
H	-7.01557	-2.16874	1.48839
O	1.21921	-2.72521	-0.65836
C	1.34911	-4.10397	-0.28921
H	1.74382	-4.20173	0.72668
H	0.38078	-4.60959	-0.33635
H	2.04007	-4.54	-1.01336

S	-0.86538	3.81764	0.21839
O	0.0757	4.41015	1.17231
O	-2.31383	3.90447	0.42445
N	-0.4746	2.19236	0.07479
C	-0.51801	4.57071	-1.39533
H	-0.7579	5.6332	-1.31468
H	0.54046	4.4411	-1.63115
H	-1.14691	4.10189	-2.15538
O	2.50763	0.04346	0.26155
N	5.42778	-0.7169	-0.09925
C	5.30512	0.55795	0.70498
H	5.82681	1.35247	0.16629
H	4.22087	0.74976	0.79104
H	5.7753	0.39428	1.67738
C	6.86313	-1.08691	-0.28063
H	7.31992	-1.23882	0.6995
H	6.92398	-2.0078	-0.86433
H	7.37684	-0.27991	-0.80727
C	4.68409	-1.8124	0.6309
H	4.76385	-2.72885	0.04198
H	5.15468	-1.95065	1.60708
H	3.64217	-1.45729	0.71288
C	4.7611	-0.50183	-1.43944
H	5.29388	0.29791	-1.9594

H	4.83242	-1.43132	-2.00878
H	3.71479	-0.23271	-1.21317

TS (3R*,4S*,5R*)

C	-0.73874	-0.53498	1.09443
C	-0.87585	-1.13757	-0.31251
C	-2.11101	-0.78495	-1.05175
C	-1.58068	1.49667	-1.19151
C	-1.69996	1.67264	0.32953
H	-0.01554	-0.84169	-0.91904
H	-1.61133	-0.82292	1.68779
H	0.1751	-0.90083	1.5634
H	-1.58351	2.74067	0.54961
H	-2.67825	1.3386	0.69043
H	-2.08596	-1.00869	-2.11458
S	-0.65121	-3.04429	-0.14365
C	-3.41104	-0.88394	-0.45329
O	-3.71075	-0.84206	0.74623
C	-2.7851	1.95671	-1.99386
H	-2.69977	1.59195	-3.02051
H	-3.73532	1.61955	-1.57548
H	-2.78677	3.0581	-2.02842
C	1.13383	-3.16949	-0.01954
C	1.75612	-3.41804	1.21346
C	1.93661	-3.03443	-1.1654

C	3.14591	-3.52522	1.30032
H	1.142	-3.53037	2.10197
C	3.32617	-3.13345	-1.07554
H	1.45879	-2.8707	-2.1274
C	3.93541	-3.37943	0.15844
H	3.61129	-3.72104	2.26302
H	3.93312	-3.04308	-1.97402
H	5.01672	-3.46809	0.22669
O	-4.40892	-0.9409	-1.4113
C	-5.73659	-0.98239	-0.8949
H	-5.8898	-1.86298	-0.26252
H	-5.96521	-0.09175	-0.29945
H	-6.39268	-1.02848	-1.76744
S	0.16287	1.70928	2.27485
O	0.27916	3.13802	1.93427
O	1.38595	0.94582	2.57075
N	-0.61826	0.94866	1.01945
C	-0.90332	1.58993	3.73092
H	-0.38373	2.07003	4.563
H	-1.84379	2.10313	3.52011
H	-1.0819	0.53537	3.95046
O	-0.43652	1.54554	-1.71786
N	2.76637	2.22864	-1.42514
C	2.387	1.9826	-2.86325

H	1.31841	1.75485	-2.88913
H	2.61107	2.88291	-3.43984
H	2.97684	1.14345	-3.23772
C	2.44607	0.99041	-0.6181
H	3.01259	0.15127	-1.02704
H	2.71038	1.16403	0.42549
H	1.36992	0.83254	-0.70868
C	1.94371	3.38117	-0.89843
H	2.21472	4.27833	-1.45969
H	0.89567	3.11353	-1.04507
H	2.14528	3.50805	0.1651
C	4.22409	2.54575	-1.31812
H	4.80083	1.69601	-1.68842
H	4.44331	3.4344	-1.91366
H	4.46692	2.72957	-0.27025

TS (3R*,4R*,5S*)

C	-1.35387	1.22927	-0.81272
C	-1.21593	-0.23891	-0.39412
C	0.21298	-0.72652	-0.40544
C	1.37863	0.51219	0.56638
C	0.91745	1.85496	-0.0428
H	-1.64314	-0.37792	0.60029
H	-1.0508	1.3382	-1.86823
H	-2.39501	1.5391	-0.71687

H	1.43035	2.65158	0.50362
H	1.25196	1.87878	-1.09313
H	0.69178	-0.67274	-1.38484
S	-2.29126	-1.27059	-1.5533
C	0.38509	-2.04152	0.22499
O	-0.29443	-2.50853	1.12807
C	0.99543	0.36645	2.03975
H	1.57148	1.1015	2.61908
H	-0.06618	0.54749	2.22692
H	1.25131	-0.63261	2.40338
C	-3.79985	-1.47924	-0.60395
C	-5.02293	-1.07674	-1.15592
C	-3.77725	-2.09766	0.65584
C	-6.21276	-1.2924	-0.45748
H	-5.0375	-0.59206	-2.12779
C	-4.96801	-2.28793	1.35658
H	-2.82894	-2.42368	1.07452
C	-6.18815	-1.89208	0.80214
H	-7.15718	-0.97703	-0.89403
H	-4.94282	-2.75973	2.33572
H	-7.11363	-2.04962	1.34991
O	1.46985	-2.7273	-0.26571
C	1.68002	-4.00685	0.33846
H	1.89733	-3.91051	1.40705

H	0.79782	-4.64262	0.22278
H	2.53186	-4.4477	-0.18534
S	-1.061	3.65927	0.31156
O	-0.15166	4.27274	1.28373
O	-2.50458	3.60116	0.55296
N	-0.52893	2.08791	0.05159
C	-0.82592	4.54218	-1.25568
H	-1.16378	5.56968	-1.10349
H	0.23419	4.53002	-1.51836
H	-1.42531	4.06212	-2.03234
O	2.62687	0.24796	0.27328
N	5.55361	-0.55786	-0.26369
C	5.40756	0.04577	1.11432
H	6.03518	0.93828	1.16566
H	4.34016	0.28388	1.23191
H	5.74431	-0.69098	1.84692
C	6.97995	-0.92176	-0.52354
H	7.30555	-1.64676	0.22505
H	7.0609	-1.35796	-1.52116
H	7.59563	-0.0222	-0.46069
C	4.6734	-1.78431	-0.34695
H	4.76567	-2.20389	-1.35096
H	5.02614	-2.50558	0.39371
H	3.64638	-1.45699	-0.14017

C	5.07395	0.44726	-1.28527
H	5.70412	1.33654	-1.21163
H	5.17357	-0.00045	-2.27656
H	4.02468	0.66342	-1.03449

TS (3R*,4S*,5S*)

C	-1.48299	0.51572	-0.63755
C	-1.18839	-0.73026	0.20691
C	0.27264	-1.11396	0.27061
C	1.33042	0.52352	0.80411
C	0.73373	1.56453	-0.15882
H	-1.54197	-0.54535	1.22447
H	-1.2017	0.32337	-1.67936
H	-2.54653	0.75049	-0.57754
H	1.15434	2.53663	0.11465
H	1.06134	1.30633	-1.17533
H	0.49127	-1.80732	1.08144
S	-2.22061	-2.18312	-0.41635
C	0.92946	-1.51574	-0.97334
O	0.71705	-1.09351	-2.10326
C	0.91527	0.69904	2.26522
H	1.38259	1.61742	2.64918
H	-0.16394	0.79532	2.40465
H	1.28766	-0.14227	2.85883
C	-3.86706	-1.75116	0.15602

C	-4.86287	-1.41054	-0.77015
C	-4.18999	-1.79497	1.52075
C	-6.15798	-1.1179	-0.33819
H	-4.6151	-1.37592	-1.82687
C	-5.48003	-1.4851	1.95033
H	-3.42802	-2.0795	2.24094
C	-6.46821	-1.14896	1.02194
H	-6.92169	-0.85547	-1.06588
H	-5.7167	-1.51593	3.01088
H	-7.47445	-0.91306	1.35797
O	1.93724	-2.427	-0.74693
C	2.61679	-2.85643	-1.92497
H	1.92398	-3.32218	-2.63238
H	3.10567	-2.0182	-2.4335
H	3.35758	-3.58919	-1.59352
S	-1.41682	3.18393	-0.28384
O	-0.56516	4.14454	0.42602
O	-2.845	3.0723	0.02508
N	-0.734	1.66542	-0.08646
C	-1.28975	3.57366	-2.05034
H	-1.73113	4.56156	-2.19971
H	-0.23658	3.5827	-2.3393
H	-1.84087	2.82445	-2.62269
O	2.60113	0.31894	0.60438

N	5.62851	-0.27341	0.49512
C	5.34635	0.84436	1.47182
H	5.87488	1.73799	1.13272
H	4.2569	0.98573	1.46935
H	5.71507	0.54165	2.45429
C	5.11212	0.13338	-0.86668
H	5.30646	-0.68474	-1.56322
H	4.0357	0.32107	-0.74999
H	5.65165	1.02934	-1.1819
C	4.88239	-1.50907	0.94731
H	5.24944	-1.78258	1.93905
H	3.81751	-1.24365	0.95993
H	5.08725	-2.31159	0.23643
C	7.09681	-0.54774	0.43137
H	7.61563	0.35626	0.10616
H	7.44873	-0.84116	1.42236
H	7.27791	-1.35571	-0.28021

TS (3R*,4R*,5R*)

C	0.53322	-1.01517	-2.10965
C	0.80245	0.29053	-1.3523
C	-0.11227	1.41268	-1.73938
C	-2.04014	0.63573	-1.41205
C	-1.91545	-0.60587	-2.31765
H	0.72818	0.10461	-0.28128

H	0.68925	-0.86398	-3.18576
H	1.24276	-1.77951	-1.78455
H	-2.86214	-1.15437	-2.27066
H	-1.73665	-0.32135	-3.36173
H	-0.08877	1.69673	-2.79179
S	2.62935	0.73792	-1.64355
C	-0.10859	2.5375	-0.82413
O	0.13583	2.49652	0.38222
C	-2.92857	1.71068	-2.04083
H	-2.87901	2.63359	-1.45882
H	-2.65622	1.93995	-3.07639
H	-3.96964	1.35522	-2.02539
O	-2.17558	0.40919	-0.15992
C	3.42207	0.17093	-0.1381
C	4.47386	-0.75229	-0.20935
C	3.04923	0.69602	1.11011
C	5.14572	-1.14628	0.95004
H	4.76199	-1.15892	-1.17447
C	3.71259	0.28278	2.26537
H	2.24676	1.42782	1.1576
C	4.76399	-0.63529	2.19095
H	5.96243	-1.8608	0.88191
H	3.42092	0.69571	3.22865
H	5.2843	-0.94599	3.09336

O	-0.50566	3.70738	-1.42144
C	-0.57679	4.83936	-0.55602
H	0.39414	5.04233	-0.09332
H	-0.87607	5.67783	-1.18841
H	-1.31387	4.68719	0.23967
S	-1.11055	-2.67239	-0.7527
O	-2.56164	-2.83508	-0.58937
O	-0.26082	-2.45936	0.43425
N	-0.83861	-1.53236	-1.94848
C	-0.49459	-4.17984	-1.53812
H	-0.59936	-4.9871	-0.80964
H	-1.09801	-4.37831	-2.42484
H	0.55642	-4.05341	-1.8043
N	-2.0727	0.04202	2.99521
C	-2.07399	-0.14926	4.47721
H	-3.10541	-0.1765	4.83491
H	-1.5744	-1.09103	4.7122
H	-1.53984	0.68025	4.94466
C	-2.81862	-1.09239	2.33029
H	-2.82253	-0.90129	1.25469
H	-2.29367	-2.02326	2.54576
H	-3.8308	-1.11684	2.74128
C	-0.65077	0.07715	2.48172
H	-0.70133	0.30665	1.41812

H	-0.11605	0.86171	3.01934
H	-0.19634	-0.89949	2.64704
C	-2.74109	1.34537	2.63323
H	-2.71213	1.42032	1.5401
H	-3.76542	1.32351	3.01287
H	-2.18157	2.15959	3.09794

GS (3R*,4R*,5R*)

C	0.64673800	-1.24585100	-1.88781900
C	0.94212500	0.06658000	-1.14873900
C	0.07822600	1.22746000	-1.65950200
C	-1.48623100	0.81760700	-1.58458500
C	-1.63446600	-0.49441000	-2.41478500
H	0.76381600	-0.06481300	-0.08229400
H	0.97686200	-1.16458800	-2.93190400
H	1.21542000	-2.05864400	-1.42964400
H	-2.67496600	-0.81761400	-2.35878700
H	-1.36876100	-0.35434400	-3.47351400
H	0.33749200	1.46621300	-2.69851400
S	2.75492200	0.46061700	-1.36118900
C	0.31108000	2.45609400	-0.81533200
O	0.50341900	2.47775900	0.38660700
C	-2.33330000	1.89680800	-2.30691000
H	-2.27246300	2.84869100	-1.77102300
H	-2.02940600	2.07347800	-3.34774500

H	-3.38195100	1.57569200	-2.29969500
O	-1.86939900	0.62215500	-0.30761200
C	3.47572000	-0.12980700	0.17280800
C	4.52366100	-1.05793100	0.12210600
C	3.06012100	0.37937300	1.41259200
C	5.15055100	-1.47432100	1.29851700
H	4.84214400	-1.45255000	-0.83838400
C	3.67730200	-0.05828800	2.58413300
H	2.26314400	1.11682400	1.44506900
C	4.72533400	-0.98133400	2.53246600
H	5.96411800	-2.19366600	1.24862700
H	3.34944200	0.33724100	3.54259700
H	5.20855400	-1.31147400	3.44834900
O	0.24630400	3.59165900	-1.55580600
C	0.42767500	4.81159400	-0.82711700
H	1.40136300	4.82192000	-0.32927300
H	0.36889500	5.60930300	-1.56903100
H	-0.35489600	4.93485500	-0.07247500
S	-1.36164400	-2.60828700	-0.71878100
O	-2.83007400	-2.56215100	-0.73085800
O	-0.62821200	-2.46492200	0.55269000
N	-0.78318400	-1.59064800	-1.92266300
C	-0.88588400	-4.22363500	-1.37923400
H	-1.18881800	-4.97360400	-0.64489700

H	-1.40547400	-4.37677500	-2.32590700
H	0.19601100	-4.25877400	-1.52124800
N	-2.71463300	0.42831700	2.65548100
C	-3.12830600	0.30872700	4.08429700
H	-4.18791200	0.55796300	4.17375500
H	-2.95966600	-0.71744500	4.41704500
H	-2.53298400	0.99656600	4.68851800
C	-3.52606400	-0.51409700	1.79380700
H	-3.20395000	-0.34829200	0.75724300
H	-3.31324000	-1.53723000	2.10531300
H	-4.58316200	-0.27987600	1.94366000
C	-1.24741700	0.09248500	2.50410400
H	-1.01235600	0.24311400	1.44391700
H	-0.67988600	0.76595500	3.15001300
H	-1.09806900	-0.94823700	2.79234500
C	-2.92835500	1.83512100	2.15381900
H	-2.59597400	1.82950600	1.10424700
H	-3.98966700	2.07697500	2.25077900
H	-2.32875600	2.51361000	2.76471600

Bibliography

[1] K.N. Houk, J. Gonzalez, Y. Li, *Acc. Chem. Res.*1995,28,2,81-90.

[2] A.Simon, Yu-hong Lam, K.N. Houk, *J.Am. Chem. Soc.* 2016,138,2,503-506.

[3] L.Simòn, J.M.Goodman, *J.Am. Chem. Soc.* 2008, 130, 27, 8741-8747.

[4] H. Tse-Lok, *Chemical Review.*1974, 75, 1, 1-20

[5} C. Cheng, J.Xu, R. Zhu, L. Zing, X. Wang, Y. Ju *Tetrahedron*, 2009, 65, 8538-8541.

[6] J. Cossy, C. Dummas, D. Gomez Pardo *Eur. J. Org. Chem.* 1999, 1693-1699

[7] F. Serpier, J-L, Bayers, B. Follèas, S. Darses *Org. Lett.* 2015, 17, 5496-5499

[8] R. Wijtmans, M. K. S. Vink, H. E. Schoemaker, F. L. van Delft, R. H. Blaauw, F. P. J. T Rutjes, *Synthesis*, 2004, 641-662

[9] M. Penso, V. Lupi, D. Albanese, F. Foschi, D. Landini, A. Tagliabue *Synlett* 2008, 2451-2454.

[10] M. L. Leathen, B. R. Rosen, J. P. Wolfe *J. Org. Lett*, 2009, 74 14, 5107-5110

[11] M.U. Luescher, C-V. T Vo, J.W- Bode *Org. Lett,* 2012, 14, 17, 4482-4485.

[12] C.F. Sequeira, S.R. Chemler, *Org. Lett,* 2012, 14,17, 4482-4485.

[13] G.Bertuzzi. F. Silvestrini, P. Moimare, D. Pecorari, A. Mazzanti, L. Bernardi, M. Foschi, *Advance Synthesis & Catalysis,* 2020, 362, 1167-1175

[14] N. L. Allinger, Y. H. Yuh, J. H. Lii, *J. Am. Chem. Soc,* 1989, 111,23, 8551-8566.

[15] S. M. Bachrach, *Computational Organic Chemistry*, 2007, 279-339.

[16] P. Hohenberg, W. Kohn, *Physical Review*, 1964, 136, B864.

[19] W. Kohn, L. J. Sham, *Physical Review*, 1965, 140, A1133

[18] R.G. Parr, W. Yang, *Density-functional theory of atoms and molecules*, Oxford University Press, New York, 1989.

[19] Y. Zhao, D. G. Truhlar, *Theor. Chem. Account*, 2008, 120:215-241.

[20] R. Ditchfield, W. J. Hehre, J. A. Pople, *The Journal of Chemical Physics*, 1971, 54, 724.

[21] S. Glasstone, K. Laidler, H.Eyring, *The Theory of Rate Processes*, McGraw-Hill, New York 1941.

[22] K. Fukui, *Account of Chemical Research*, 1981, 14, 12, 363-368.

[24] B. Podolsky, *Physical Review*, 1928, 32, 812.

[25] Hammond, G. S. A Correlation of Reaction Rates. *J. Am. Chem. Soc.* 1955, *77*, 334-338.

[26] a) Y. Zhao, D.G Truhlar, *Phys. Chem. Chem. Phys*. 2008, 10, 2813-2818; b) R. F. Ribeiro, A. V. Marenich, C. J. Cramer, D. G. Truhlar, *J. Phys. Chem.* B 2011, 115, 14556-14562; c) S. Grimme, *Chemistry-Eur. J.* 2012, 18, 9955-9964.

[27] P. Moimare, *Sintesi e caratterizzazione strutturale di derivati piperidinici e morfolinici chirali*, 2019, Università di Bologna, Corso di studi in Chimica Industriale.

[28] N. Yoneda, Y. Fujii, A. Matsumoto, K. Asano, S. Matsubara, *Nat. Commun.* 2017, 8, 1397.

[29] Gaussian 16, rev A.03. M. J. Frisch, G. W. Trucks, H. B. Schlegel, G. E. Scuseria, M. A. Robb, J. R. Cheeseman, G. Scalmani, V. Barone, G. A. Petersson, H. Nakatsuji, X. Li, M. Caricato, A. V. Marenich, J. Bloino, B. G. Janesko, R. Gomperts, B. Mennucci, H. P. Hratchian, J. V. Ortiz, A. F. Izmaylov, J. L. Sonnenberg, D. Williams-Young, F. Ding, F. Lipparini, F. Egidi, J. Goings, B. Peng, A. Petrone, T. Henderson, D. Ranasinghe, V. G. Zakrzewski, J. Gao, N. Rega, G. Zheng, W. Liang, M. Hada, M. Ehara, K. Toyota, R. Fukuda, J. Hasegawa, M. Ishida, T. Nakajima, Y. Honda, O. Kitao, H. Nakai, T. Vreven, K. Throssell, J. A. Montgomery, Jr., J. E. Peralta, F. Ogliaro, M. J. Bearpark, J. J. Heyd, E. N. Brothers, K. N. Kudin, V. N. Staroverov, T. A. Keith, R. Kobayashi, J. Normand, K. Raghavachari, A. P. Rendell, J. C. Burant, S. S. Iyengar, J. Tomasi, M. Cossi, J. M. Millam, M. Klene, C. Adamo, R. Cammi, J. W. Ochterski, R. L. Martin, K. Morokuma, O. Farkas, J. B. Foresman, and D. J. Fox, Gaussian, Inc., Wallingford CT, 2016.

[30] Gausswiew 6.0.16.